

DOI: 10.1002/
Review Article

Epoxy-based Nanocomposites for High-Voltage Insulation: A Review

*Mohammed Mostafa Adnan**, *Erlend Grytli Tveten*, *Julia Glaum*, *Marit-Helen Glomm Ese*,
Sverre Hvidsten, *Wilhelm Glomm*, *Mari-Ann Einarsrud**

M. M. Adnan, Dr. J. Glaum, Prof. M.-A. Einarsrud

Department of Materials Science and Engineering, NTNU Norwegian University of Science and Technology, 7491 Trondheim, Norway.

Email: mari-ann.einarsrud@ntnu.no

Dr. E. G. Tveten, Dr. M.-H. G. Ese, Dr. S. Hvidsten

SINTEF Energy Research AS, Sem Saelands vei 11, 7034 Trondheim, NORWAY

Dr. W. Glomm

SINTEF Industry, 7465 Trondheim, Norway

Keywords: epoxy nanocomposites, high-voltage insulation, structure-property relations

Abstract

Epoxy nanocomposites, with inorganic oxide nanoparticles as filler, can exhibit novel property combinations, such as enhanced mechanical strength, higher thermal conductivity, increased dielectric breakdown strength, and reduced complex permittivity. Therefore, they have interesting applications as nanodielectrics, such as high-voltage insulation materials or in microelectromechanical systems. The primary challenge in the processing of nanocomposites is achieving a homogeneous dispersion of the nanoparticles. The dispersion quality affects the

This is the peer reviewed version of the following article: Adnan, Mohammed Mostafa, et al. "Epoxy-Based Nanocomposites for High-Voltage Insulation: A Review." *Advanced Electronic Materials* (2018): 1800505, which has been published in final form at <https://doi.org/10.1002/aelm.201800505>. This article may be used for non-commercial purposes in accordance with Wiley Terms and Conditions for Use of Self-Archived Versions

interfaces between the organic and inorganic components, which can determine the final properties of the nanocomposite. In this review the processing methods and the resulting dielectric, mechanical and thermal properties of epoxy nanocomposites with inorganic oxide fillers are presented. Functionalization of the nanoparticle generally improves the dispersion of the particles in the polymer matrix. Different oxide fillers are observed to have similar effects on the properties of the nanocomposites. Epoxy-based nanocomposites exhibit improved dielectric breakdown strength and lower complex permittivity with inorganic oxide nanoparticles at low filler contents, compared to conventional composites with micron-sized particles. While there are some inconsistencies in the findings, which may be attributed to differences in the dispersion quality, an improved understanding of the nanoparticle-epoxy interfaces in the nanocomposites will enable tailoring of properties, potentially opening new avenues for application.

1. Introduction

Nanocomposites are a class of hybrid organic-inorganic materials, where inorganic nanoparticles are dispersed in an organic polymer matrix. The use of nanoparticles instead of micron-sized particles has shown promising improvements of the electrical, mechanical and thermal properties of the polymer.^[1-5] The improved properties enable the use of polymer nanocomposite systems in a wide range of applications, such as nanodielectrics in microelectronics, coatings, proton exchange membranes, catalysts, and packaging materials.^[5]

^{6]} Recently, there has been increased interest in nanocomposites as high-voltage insulation materials, with epoxy as one of the most important polymer base materials.

Electrical insulation systems are imperative in power components. The insulating materials should typically have a high dielectric breakdown strength and thermal conductivity that facilitates high power ratings. Exposure of the insulation to various environmental and operational stresses can result in local degradation and eventually to an electrical breakdown, which is catastrophic for power system transmission reliability.

Epoxy-based composites are increasingly attractive due to high tensile strength, good adhesion and excellent resistance against chemical corrosion.^[7, 8] Epoxy is frequently used as electrical insulation in power equipment, such as dry-type (cast resin) transformers and rotating machines,^[2, 9, 10] as well as in printed circuit boards, gas insulation switchgear (GIS) spacers and generator groundwall insulation systems.^[10] However, epoxy is also brittle, and may be improved by physical reinforcement from filler materials.^[5, 11] The addition of microparticle fillers to epoxy can result in improvements in the mechanical properties (e.g. fracture toughness and thermal expansion) and decreased water absorption,^[12] but at the cost of reduced electric breakdown strength and increased complex permittivity.^[13] The use of nanoparticles instead of microparticles has shown promising potential for improved mechanical properties while retaining the excellent dielectric performance of epoxy composites.

However, variations in the results presented by different studies make it challenging to assess the general performance of different nanocomposites.^[14] For example, the inclusion of nanoparticles has been shown to increase as well as decrease the complex permittivity,^[13, 15] breakdown strength^[10, 16] and glass transition temperature^[7, 10] of epoxy nanocomposites. These conflicting results, along with variations in the processing methods, make it difficult to determine the real effect of the different nanoparticles on the properties of the resulting composites. There is a general agreement in the literature that improved dispersion of the

nanoparticles can lead to improvements in the desired properties for high voltage insulation (e.g. increased breakdown strength, glass transition temperature and fracture toughness, and decreased permittivity and dielectric loss). However, due to the lack of a proper quantitative analysis scheme for the state of dispersion in many of the studies, it is challenging to determine exactly how the nanoparticles affect the properties of the composite. The particle size, the modification of the particle surface, and the methods used in the preparation of the materials can greatly affect the quality of dispersion. In addition, several studies have reported an improved dispersion of nanoparticles with functionalized or chemically modified surfaces.^[17] Other advantages with surface modification that have been reported are a reduction in water absorption,^[1, 18] increased tensile strength and fracture toughness,^[7, 12] as well as improved permittivity and breakdown strength.^[19] However, it is still unclear if it is the improved dispersion itself, or the change in interactions caused by the functionalization that leads to changes in the properties of the nanocomposites.

In this review, a brief overview of the structure and properties of epoxy and selected inorganic oxides as filler is provided, followed by a general introduction to the chemistry of the particle surface and the interfaces between the particles and the polymer. Subsequently, the reported methods for the preparation of epoxy-based nanocomposites are discussed, followed by an outline of several quantitative techniques for characterizing the state of dispersion. Finally, several studies investigating the properties of epoxy-based nanocomposites are reviewed. The changes in the dielectric, mechanical and thermal properties of the nanocomposites are compared and discussed. Connections between the preparation methods, the resulting states of dispersion, and the changes in properties observed in the different studies are highlighted in

order to better understand how various factors affect the properties of the nanocomposite materials.

2. The Structure of epoxy nanocomposites

2.1 The epoxy resin

Epoxy is a thermoset, a network polymer with covalent crosslinks between the monomers that becomes permanently hard upon curing.^[11] Unlike thermoplastics (e.g. polyethylene), thermosets do not soften upon heating, making them generally stronger but also more brittle. The chain length of the monomer and the molecular mass affects the degree of interaction with the nanoparticles. Most of the studies investigating the dielectric properties of epoxy uses diglycidyl ether of bisphenol-A (DGEBA) (**Figure 1**) as the epoxy resin. Cycloaliphatic epoxies (e.g. 3,4-epoxycyclohexylmethyl 3,4-epoxycyclohexanecarboxylate) are also used in some cases. **Table 1** summarizes selected properties of DGEBA.

2.2 The filler materials

2.2.1 Oxide fillers

Inorganic oxides are typically used as filler materials in epoxy-based nanocomposites for high voltage insulation applications. Nanoparticles of titanium dioxide (*titania*, TiO_2), silicon dioxide (*silica*, SiO_2), and aluminium oxide (*alumina*, Al_2O_3) feature most often in the literature, and therefore epoxy nanocomposites containing oxides are the focus of this review. Selected properties of these oxides are shown in **Table 2**.

TiO_2 is a wide band gap, ionic semiconductor that exists in several polymorphs.^[28, 29] Primary among these are the rutile, anatase and brookite phases (**Figure 2**). The rutile phase is more

stable in bulk. For nanoparticles below 30 nm anatase is stable over rutile due to lower surface energy.^[30] However, between 30 and 200 nm, there is no strong preference and either rutile or anatase may form. For nanodielectrics, the distinction between rutile and anatase may become important because of the difference in the relative permittivity (dielectric constant) of the two phases, which is due to a polaron effect. There is greater structure distortion and more ionic Ti-O bonds in rutile, which results in greater ionic screening and larger effective electron masses, resulting in a higher relative permittivity.^[31]

SiO₂ is an electrical insulator that is typically amorphous when used as a nanofiller for property enhancement in composites.^[34] The structure consists of tetrahedral SiO₄ units bridged by O atoms and lacks the long-range order present in crystalline forms. Alumina (Al₂O₃) is an electrical insulator that commonly occurs in the corundum structure (α -Al₂O₃).^[35] However, nano-sized Al₂O₃ may also exist in an amorphous phase (composed of varying fractions of AlO₄, AlO₅ and AlO₆ polyhedra) as the surface energy is lower than for α -Al₂O₃ when the surface area exceeds 370 m² g⁻¹.^[36]

2.2.2 Non-oxide fillers

The scope of this review will be focused on inorganic oxide nanofillers for epoxy nanocomposites, due to their prevalence in the literature. However, while the inorganic oxides are most frequently used in studies of the dielectric properties of epoxy nanocomposites, other nanoparticles have been investigated as well. Aluminium nitride (AlN) and boron nitride (BN) are non-oxide nanofillers that are used due to their intrinsic high thermal conductivities.^[42] The addition of cubic BN in epoxy modified with polyhedral oligomeric silsesquioxanes (POSS) has led to improved dielectric breakdown strengths, enhanced thermal conductivities, and

higher glass transition temperatures.^[43, 44] Hexagonal BN and AlN in epoxy nanocomposites have also shown to decrease the permittivity for low filler contents.^[20, 44] Silicon carbide (SiC) is another non-oxide alternative nanofillers in epoxy, exhibiting improved partial discharge resistances.^[45] For an overview of other nanoparticles and polymer systems in high voltage insulation applications, the reader is referred to other works with a broader focus.^[5, 42]

2.3 The nanoparticle interface

The size and surface chemistry of the nanoparticles influences their arrangement and structure within the polymer matrix. The interface between the nanoparticles and the surrounding polymer chains is believed to be an important factor for the properties exhibited by the nanocomposite.^[1, 3, 13, 14] Smaller particles possess a larger surface area to volume ratio due to a greater fraction of surface atoms.^[46] As a result, nanoparticles possess a significantly higher surface energy than micron-sized particles, and will tend to form clusters or agglomerates to reduce the total surface area and minimize the available surface energy. Agglomerate formation is further driven by the incompatibility between the hydrophilic inorganic particles and the hydrophobic organic polymer chains, and the large difference in surface energy between them.^[47] Composite materials consisting of well-dispersed nanoparticles will therefore have a larger area available where the polymer chains and inorganic particles can interact, compared to the micron-sized counterparts. These interactions between the particles and the polymer are suspected to alter the behavior of the polymer chains around the particle, forming the interfacial region.

Composites with agglomerated nanoparticles will most likely behave similar to traditional microcomposites if the agglomerates become large. For larger particles or agglomerates, the Lichteneker-Rother logarithmic law of mixing can be applied to predict the properties of the composite.^[3, 13] This method is not applicable when the particles are nano-sized and well dispersed in the polymer because the interfacial region comprises a larger part of the total volume. For example, for epoxy-TiO₂ microcomposites (10 wt%) the permittivity increased significantly, which is expected due to TiO₂ having a much higher permittivity than epoxy.^[1, 13] However, for an epoxy-TiO₂ nanocomposite the permittivity decreased instead.^[13] This decrease led to speculations that the dielectric properties of the interfacial region may be drastically different from those of either the polymer or the inorganic filler, and that a large interfacial region is responsible for the drop in permittivity of the nanocomposite.^[20]

Tsagaropoulos and Eisenberg^[48] proposed a model for the interface between the polymer chains and the nanoparticles, where the interactions between the particles and the chains cause regions with restricted chain mobility. This region could be split into two layers: a tightly bound layer (which does not contribute to the glass transition), and a loosely bound layer (which may exhibit its own glass transition unique from the rest of the polymer). The loosely bound layers of neighboring nanoparticles may overlap.

Tanaka et al.^[49] on the other hand proposed a multi-core model for the interface, consisting of three layers instead: an inner bonded layer, then a bound layer and finally an outer loose layer. In addition, they also proposed the presence of an electric double layer^[50] that overlaps the other three layers when Coulombic interaction is superimposed. The bonded layer (~1 nm thick) is a transition region where the polymer chains are chemically bonded to the nanoparticle surface by coupling agents (see **Chapter 2.4**). This layer forms only when such coupling agents

are used to functionalize the nanoparticle surface, and may indirectly affect the properties of the nanocomposite. The bound layer (~2-9 nm thick) consists of polymer chains that interact strongly with the first layer. The loose layer (>10 nm thick) consists of polymer chains that interact weakly with the second layer. The chain mobility, conformation and crystallinity in the polymer matrix vary in the different layers of the interfaces.^[49] **Figure 3** displays a comparison of the two models.

The formation of bonded and bound layers in these models may be seen as a parallel to the electrical double layer for colloidal dispersions,^[50] with the bonded layer corresponding to the Stern layer and the bound layers corresponding to the diffuse Guoy-Chapman layers.

2.4 Surface functionalization of the nanoparticles

Functionalization of the nanoparticle surface with organic molecules is a common approach to improve their dispersibility in the polymer matrix,^[51] either via steric repulsion or a reduction in the surface energy by forming bonds with the polymer chains. These bonds may also reduce the hydrophilic nature of the inorganic nanoparticles and improve compatibility with the organic matrix. The surface modification can be done physically (e.g. using surfactants or macromolecules adsorbed on the nanoparticle surface) or chemically (e.g. using coupling agents that form chemical bonds with the nanoparticle surface atoms). Since physical modification may be thermally and solvolytically unstable due to the weak forces (van der Waals or Hydrogen bonds) that attach the molecules to the surface,^[52] chemical modifications result in more stable dispersions. Commonly used coupling agents for functionalization include silanes, carboxylates and amines.^[51-54] Silane coupling agents (SCAs) are typically used for metal oxide nanoparticles in epoxy-based nanocomposites.^[51, 52, 54] SCAs are organosilicon compounds with two different functional groups with the formula $X(\text{CH}_2)_n\text{SiR}_3$, where X is a

functional organic group and R is a hydrolysable group.^[52] The functional organic group can react with the polymer chains and the hydrolysable group can react with the surface of the inorganic particles. Some commonly used SCAs include 3-aminopropyltriethoxysilane (APTES), 3-glycidyloxypropyltrimethoxysilane (GPTMS), and 3-isocyanatopropyltriethoxysilane (IPTES),^[51, 52, 54] which are shown in **Figure 4**.

In addition to coupling agents, ligand engineering can also be used to graft ligands onto the particle surface to control the dispersion, either by providing steric hindrance or by making the particle surface hydrophobic and thus enhancing the miscibility.^[5] The ligands are short organic molecules or polymer brushes that chemically bond to the nanoparticle surface, but not to the polymer chains. Controlling the chain length and grafting density will allow tuning of the interfacial (and therefore also the bulk) properties of the nanocomposite,^[23] and is investigated further in **Chapter 4.1.2**.

3. Preparation of epoxy nanocomposites

3.1 Methods and procedures

In most studies investigating the dielectric properties of nanocomposites, an *ex situ* approach is normally used for the fabrication of the samples. This involves the incorporation of pre-synthesized nanoparticles either directly into the polymer (blending) or into a monomer solution that is subsequently polymerized (*in situ* polymerization).^[55] These methods are most practical for large-scale production and industrial application as of today. If the nanoparticles were unmodified by the supplier, the surface functionalization can be applied prior to mixing with epoxy. **Figure 5** shows a schematic of the two different approaches. The blending route involves dispersing the nanoparticles in the resin using either physical force (via mechanical or high-shear mixers), ultrasonication, or a combination of the two. This direct mixing may be

done at temperatures above the softening point of the polymer (melt compounding), or by mixing the particles and the polymer in a common solvent (solution mixing).^[5, 56] After the dispersion, the nanocomposite resin can be cast using a mold or deposited onto a substrate to form coatings or thin films after curing. *In situ* polymerization is more effective for preparing larger bulk samples, as it can be applied directly to polymer extrusion, which facilitates industrial production.^[1] The process involves mixing the nanoparticles with a monomer solution, followed by the polymerization reaction. However, this process requires a longer time for the polymerization.^[1] Figure 6 shows that in the epoxy-CaCO₃ nanocomposites prepared by solution mixing, the agglomerates are larger than those prepared by *in situ* polymerization. This is expected since in blending procedures where the organic matrix is already polymerized it is more difficult to disperse the nanoparticles, compared to dispersing them among shorter monomer units which are afterwards polymerized (*in situ* polymerization). The presence of nanoparticles increases the viscosity of the liquid epoxy,^[57] thus affecting the processability of the nanocomposite resin. This is an important consideration for fabrication of these materials at a larger (more industrial) scale. The viscosity increase is dependent on the interfacial interactions (which are affected by the surface modification). Attractive interactions between the nanoparticles and the epoxy chains, which result in an improved dispersion, led to a smaller increase in the viscosity than repulsive interactions, which result in agglomeration.^[57] **Table 3** describes the methods used for the dispersion of nanoparticles during fabrication in selected studies surveyed in this review.

3.2 Characterizing the state of dispersion

Currently, there are no agreed standards on the evaluation of the dispersion quality and which criteria should be used to characterize a ‘well-dispersed’ nanocomposite. Various studies

investigating nanocomposites show a large spread of particle and agglomerate sizes.^[10, 13, 15, 16, 20, 22, 23, 61-64] Since the state of dispersion is known to affect the materials properties, any detectable differences in dispersion quality will be considered when comparing results from different studies in this review.

Parameters that can affect the state of dispersion include the particle size and shape, particle size distribution, the surface functionalization, the type of polymer, the length of the polymer chains, and the methods used for mixing and curing. The methods commonly used for the preparation of nanocomposites summarized in Table 3 exhibit several challenges. Mechanical mixing requires high shear forces to ensure the nanoparticles are well dispersed in the viscous epoxy resin.^[1] However, using high shear forces does not guarantee that all agglomerates are broken. Ultrasonication is an alternative method.^[22] Centrifugal force may be combined with ultrasonication, as in the experiments conducted by Kurimoto et al.,^[22] resulting in a removal of heavier agglomerates from the composite. However, this method makes it difficult to control the filler content in the final nanocomposite.

The majority of studies include some qualitative assessment of whether or not the particles are agglomerated or dispersed in the polymer matrix. However, it is challenging to compare properties of different nanocomposites and from different studies based on qualitative descriptions of the state of dispersion. Quantitative dispersion characterization techniques are therefore needed to compare the effects of particle size, dispersion, filler load and processing methods on the dispersion quality.^[65] Several methods for quantitative analyses of nanoparticle dispersions have been proposed, each with advantages and disadvantages as shown in **Table 4**. Well contrasted images from various types of microscopy (TEM, SEM, AFM, etc.) are a prerequisite before such methods may be applied.

3.2.1 *Interparticle distances and deviations from uniformity*

A uniform distribution of particles, where each filler particle is equidistant from its four nearest neighbors, is often described as the theoretical optimal state of dispersion. In practice, however, a random distribution of non-agglomerated particles is perhaps the best achievable outcome for nanoparticle blending procedures. Measuring the deviation from the uniform dispersion is one approach to characterize the dispersion. However, a limitation of this approach is that the ideal ‘uniform distribution’ is size independent.^[66] In other words, it does not take into account parameters such as the filler load or particle size, which affect the size of polymer domains that are reinforced by the fillers.

The average interparticle distance (or particle separation) is also used as a characterization tool that provides a scale-dependent measure of the dispersion.^[4, 61, 62] The disadvantage of this method is that it does not provide information about how the particles are distributed, and that it is only sensitive to the number of particles.^[66] **Figure 7** shows an example with hypothetical dispersions, where both dispersions would show the same mean interparticle distance despite one of them having particles that are more agglomerated. Luo and Koo^[68] attempted to tackle this by using the distribution of interparticle distances instead of the average value. The resulting histograms using this method are shown in Figure 7. This method evaluates the dispersion quality using deviation from the average. However, this method is also scale independent and cannot describe the extent of polymer reinforcement by the nanoparticles.^[66]

3.2.2 *Particle density and the Morisita index*

Kim et al.^[67] used the particle density from TEM images together with the Morisita index to describe the dispersion state. The Morisita index is a statistical tool that was originally used for

measuring dispersion in ecological studies (e.g. for flora or fauna populations),^[69] and is calculated using Equation 1 and a single TEM image split into multiple sections.

$$I_{\delta} = Q \frac{\sum_{i=1}^Q n_i(n_i-1)}{N(N-1)} \quad (1)$$

Q is the number of sections in the TEM image, n_i is the number of particles in the i^{th} section, and N is the total number of particles. I_{δ} is greater than 1 for agglomerated particles and less than 1 for discrete particles.^[67] However, Kim et al. state that the Morisita index is not sensitive enough to compare very similar dispersions.^[67]

3.2.3 Skewness-Quadrat method

Another method used by Kim et al.^[67] (and suggested by Hui et al.^[65]) is the Skewness-Quadrat method, which is also often used in biological and ecological studies. This method involves placing a grid of square cells (or quadrats) on the TEM images (similar to the sections used in the Morisita index, but typically smaller in size and greater in number), and counting the number of particles in each cell. The skewness, β , can be calculated by Equation 2.

$$\beta = \frac{q}{(q-1)(q-2)} \sum_{i=1}^q \left(\frac{n_i - \bar{N}_q}{\sigma} \right)^3 \quad (2)$$

q is the number of cells studied, n_i is the number of particles in the i^{th} cell, \bar{N}_q is the mean number of particles per cell and σ is the standard deviation. β approaches zero when the particles are uniformly distributed, and approaches infinity for large agglomerates.^[67] Calebrese et al.^[14] used this method to give a quantitative measure of the dispersion of alumina-polyamideimide nanocomposites, and showed that a decrease in β (improved dispersion) corresponded with an increase in the electrical breakdown strength.

However, the skewness is dependent on the size of the quadrats – if the cells are chosen too small, the method will indicate agglomeration even for a dispersed system. If the cells are

chosen too large, then the converse applies, and the statistics will falsely only a small degree of agglomeration. Kim et al. used quadrats 3.5 times as large as the average particle size in their study.^[67] The selection of an optimal quadrat size is therefore an important parameter when interpreting the results.

3.2.4 Free space length

Both the Morisita index and the Skewness-Quadrat method can be useful for describing the distribution of nanoparticles, but do not provide much information about how the interfacial regions or regions of unreinforced polymer are affected. The free space length (L_f) method, developed by Khare and Burris,^[66] does not focus on the nanoparticles and their distribution, but on the regions of polymer not reinforced by nanoparticles. L_f is defined as the length of the sides of the largest randomly selected square where the most probable number of nanoparticles present is zero – in other words, it represents the characteristic size of the unreinforced polymer domains (**Figure 8**). The advantage of this method is that L_f quantitatively accounts for all the main factors that affect dispersion (particle size, distribution and load). L_f is always reduced for more uniform distribution (given constant filler size and load), for higher filler loads (given constant distribution and size) and for smaller particle sizes (given constant load and distribution). Khare and Burris reported that L_f can be modified to also be sensitive to agglomeration when the agglomerates are larger than L_f .

Agglomerates are typically described qualitatively as an aggregation or clustering of nanoparticles. However a quantitative definition is necessary. Khare and Burris defined an agglomerate as a continuous region where the spacing between individual particles is less than the characteristic particle diameter. Using this definition, the agglomerate sizes can be computed using a similar method to that used for calculating L_f .

Several studies have attempted to link changes in the measured properties of nanocomposites to various dispersion parameters, such as the interparticle distances,^[61, 62] the sizes of the filler particles prior to mixing,^[10, 15, 20] or the agglomerate sizes.^[22] However, these parameters do not separately present a description of the state and quality of dispersion. The best description of the dispersion state may be achieved by combining the various analysis techniques instead of relying on them individually.

4 The Structure-Property Relations in Epoxy Nanocomposites

4.1 Electrical properties

For high voltage insulation materials, the dielectric breakdown strength, the complex permittivity and the electrical conductivity are among the most important electrical properties. The breakdown strength indicates the maximum electric field strength the material can withstand before the insulating properties fail. The complex permittivity is a measure of how the electric field inside a material is changed (the real relative permittivity) and the associated dielectric losses. For applications in high voltage insulation systems, materials with a low relative permittivity will enable the use of larger electric fields; in other words, larger voltages (for a given thickness of insulation) or less thick insulation (for a given voltage). In this chapter, the literature on the effect of oxide nanofillers on the complex permittivity and dielectric breakdown strength of epoxy nanocomposites will be reviewed.

4.1.1 Complex Permittivity

Real relative permittivity

The use of micron-sized particles as fillers in epoxy typically increases both the dielectric losses and the relative permittivity of the final composite compared to the neat epoxy. **Figure**

9 shows a comparison of the real relative permittivity for composites containing both micron-sized and nano-sized particles of TiO₂ at different filler loads from two studies. Singha and Thomas^[10] reported a significant increase in the real part of the relative permittivity in epoxy-TiO₂ microcomposites with increasing filler content. Nelson and Fothergill^[13] also reported a higher real relative permittivity for epoxy with 10 wt% TiO₂ micron-sized particles compared to neat epoxy. However, in both studies the addition of nanoparticles decreased the permittivity, but at different filler loads. Singha and Thomas reported a slight decrease in permittivity up to 0.5 wt% nano-TiO₂ compared to neat epoxy.^[10, 15] For larger amounts of nanoparticles (5 and 10 wt%), the permittivity increased again, but was still lower than that for the equivalent amount of micron-sized particles. On the other hand, Nelson and Fothergill reported a decrease in permittivity for 10 wt% nano-sized TiO₂ from the neat epoxy, although the difference is most pronounced at lower frequencies.^[13]

Kochetov et al.^[20] investigated the effect of different types of nanoparticle fillers (SiO₂, Al₂O₃, MgO, AlN and BN) on the permittivity of epoxy, and reported similar trends for most of the materials. The relative permittivity decreased (between 2-15% from that of neat epoxy) upon addition of small amounts of Al₂O₃, MgO, and AlN nanoparticles (2-5 wt%), but increased for larger amounts (10 wt%) to above that of neat epoxy. The minimum permittivity was usually obtained at a filler load of 2 wt%, and MgO showed the largest decrease in permittivity (by 15%). An exception was observed for SiO₂ nanoparticles, which showed increased permittivity for all filler loads. This is in conflict with other studies where the addition of SiO₂ nanoparticles led to a reduction in permittivity.^[19, 70]

In all cases, the changes in permittivity between nanocomposites with different filler loads were more pronounced at lower frequencies. This might be due to a decrease in the inherent

permittivities of both the filler and the epoxy, as the dipolar groups are slower to reorient themselves when the electric field switches polarity more rapidly.

As shown from these studies, the addition of nanoparticles can reduce the permittivity of the final composite. However, the optimum load and size for the filler particles are difficult to predict. Differences in the permittivities observed for epoxy-TiO₂ (10 wt%) nanocomposites in the studies by Nelson and Fothergill^[13] and Singha and Thomas^[10] may be attributed to differences in the quality of dispersion. Both studies state that the dispersion of particles is “uniform”. However, Nelson and Fothergill reported a few agglomerates up to 500 nm in diameter, with no further information being provided on the particle dispersion. Singha and Thomas used 50 nm sized particles as filler, but did not report any agglomeration after mixing with the epoxy. Neither of the studies specified if the nanoparticle surfaces were functionalized. The differences observed in the two studies for the same filler load may alternatively be due to the use of different types of TiO₂ nanoparticles, with differences in the particle sizes (and therefore possibly differences in the crystal structures, as mentioned in **Section 2.2**).

Relative permittivities reported by Kochetov et al.^[20] of nanocomposites containing different types of fillers are presented in **Figure 10. Table 5** summarizes the changes in permittivity for the different filler types and loads, and a clear trend can be observed. The data indicates that the permittivities of nanocomposites are not strongly influence by the type of oxide filler. The size of the filler particles appears to be more influential to the permittivity of the nanocomposite than the intrinsic permittivity of the filler. Filler particles with smaller sizes (MgO, Al₂O₃) cause larger reductions in the permittivity, even if these fillers have a higher relative permittivity than fillers with larger particles (AlN). However, it should be noted that the particle sizes shown in Table 5 are given prior to mixing. TEM images after mixing show the presence

of some agglomeration of the nanoparticles, but no further details of the state of dispersion are available.

A noticeable exception to the trend of decreasing permittivity is observed for epoxy-SiO₂ nanocomposites (Table 5) where the permittivity increased for all frequencies, despite SiO₂ having a low intrinsic permittivity and the smallest particle size. This increase in permittivity is explained to be due to differences in the method of preparation and the possible presence of byproducts.^[20] The other fillers were surface modified using GPTMS prior to mixing with epoxy, but SiO₂ was obtained pre-dispersed in epoxy (as the commercial product Nanopox) with unknown surface modification, and was diluted to the required content. This shows that the surface modification of the Al₂O₃, AlN and MgO filler particles may have affected the dispersion quality differently than the commercially applied surface modification. Kochetov et al.^[20] do not include evaluations of the various dispersions of nanoparticles, or equivalent experiments without surface modification, to verify this hypothesis.

Kurimoto et al.^[22] observed a decreasing permittivity with decreasing size of the agglomerates of silane-functionalized Al₂O₃ nanofillers in bisphenol-A-epoxy. The agglomerate size was controlled by altering the duration of ultrasound and centrifugal mixing during the preparation of the nanocomposites. When the agglomerate diameter was smaller than 200 nm, the final nanocomposite possessed a lower permittivity than the neat epoxy. The decrease in permittivity with the breakdown of agglomerates may be explained by the corresponding increase in the available interfacial area. However, the downside of the preparation method used in this study is that the centrifugal mixing resulted in sedimentation and removal of heavier agglomerates, which makes it difficult to control both the filler content and agglomerate size simultaneously.

Consequently, the effect of filler load on permittivity is difficult to interpret from these results and to compare with other studies. The results from Kurimoto et al.^[22] and Kochetov et al.,^[20] however, demonstrate the importance of the particle size, and consequently the available interfacial area, to the dielectric properties of the epoxy nanocomposites with oxide fillers. In addition, Xie et al.^[25] demonstrated the effect of particle shape on the relative permittivity. Spherical nanoparticles of TiO₂ (1-4 wt%) showed a small increase in the permittivity of neat epoxy (up to 4.2 at 0.1 Hz), while TiO₂ nanowires at the same load resulted in a much larger increase in permittivity (up to 5.25 at 0.1 Hz).^[25] The specific surface areas of the nanowires and nanoparticles were measured to be 39.8 and 82.6 m² g⁻¹ respectively. Therefore, the interfacial area around the spherical nanoparticles is larger, resulting in the smaller increase in permittivity compared to the nanowires.

Studies by Bell et al.^[23] and Yeung and Vaughan^[19] demonstrate the importance of surface functionalization of the nanoparticles. Using the free space length (L_f), Bell et al.^[23] evaluated the dispersion quality of epoxy-SiO₂ nanocomposites with changing ligand graft density. Bimodal ligands were used, consisting of long polyglycidyl methacrylate (PGMA) chains attached with anthracene, thiophene and terthiophene as short, π -conjugated, electroactive surface ligands. Bell et al. showed that increasing the ligand graft density above 0.07 chains/nm² resulted in a L_f below 200 nm for 2 wt% of nano-SiO₂ in bisphenol-A epoxy.^[23] This was defined by the authors as a well-dispersed system, and the particles may have an increased surface area if they are not agglomerated.

Yeung and Vaughan^[19] also demonstrated the benefits of surface functionalization using SiO₂ nanoparticles (2 wt%) and GPTMS as a coupling agent. The relative permittivity decreased with increasing ratio of GPTMS to SiO₂, from 4.9 to 3.5 at 50 Hz.^[19] However, because no quantitative evaluation of the dispersion was given, it is difficult to conclude whether the

improvements observed can be attributed to an improvement in dispersion, or other unknown factors. Siddabattuni et al.^[4] used 5 vol% (~16 wt%) of TiO₂ nanoparticles in epoxy. The permittivity of the nanocomposites increased using unmodified particles, but the use of different bifunctional organophosphate ligands gave varying results.^[4] These changes are not significant however, and the authors concluded that the permittivity was simply dependent on the filler volume. It could be speculated that due to the much larger filler content (16 wt%) compared to that used in other studies (below 10 wt%), the ligands may no longer be equally effective in improving the quality of dispersion.

Singha and Thomas argue that the polarization mechanism in epoxy is the orientation of dipolar groups on the polymer chains.^[10] This process is reduced when the movements of the contributing groups are constrained, which occurs when there are strong interactions or bonding between the nanoparticles and the polymer chains. This results in an immobile interfacial nanolayer between the nanoparticles and the polymer.^[10, 15] The immobilization of the polymer chains is dependent on the available interfacial area, which in turn depends on the quality of dispersion and the surface chemistry. According to this model, nanocomposites with uniform dispersion, small particle sizes, and little to no agglomeration will show the lowest permittivities. The surface modification of nanoparticles may affect the interfacial interactions via formation of chemical bonds as bridges between the chains and the particles. The possibility of steric hindrance, which would prevent the polymer chains from coming close to the nanoparticles, should also be considered.

The multi-core model by Tanaka et al.^[49] predicted that the polymer chain mobility at the interfaces would be reduced by the formation of chemical bonds between the chains and the particles. This corresponds well with the results from Yeung and Vaughan,^[19] where an increasing amount of coupling agent led to increased bonding of the polymer chains and

nanoparticles, and consequently reduced the permittivity. However, since the permittivity decreased even in the absence of the silane coupling agents (e.g. in the studies by Singha and Thomas,^[10] and Nelson and Fothergill^[13]), it is possible that the polymer chains simply being loosely attached to the nanoparticle surface via weak interactions (e.g. Hydrogen bonds and van der Waal's forces, as in the case of the bound layers in both Tanaka's and Tsagaropoulos' models), can also decrease the chain mobility.

Kochetov et al.^[20] proposed that the interfacial region acts as a 'third phase' in addition to the organic (polymer) and inorganic (nanoparticle) phases in the hybrid material. In this model the 'third phase' will have properties that are different from the bulk polymer. When nanoparticles are used the interfacial region becomes larger, hence the third phase constitutes a larger volume of the composite. There will therefore be a greater number of immobilized polymer chains, and the polar groups in these immobilized chains will be less able to follow changes in the external electric field. As a result, there will be a reduced effective permittivity in this 'third phase' and consequently in the whole composite based on the logarithmic laws of mixing. One limitation with this model is that the properties (e.g. the glass transition temperature or the complex permittivity) of the interfacial region cannot be measured in isolation. While some authors agree that the immobilization of chains is a suitable model for explaining the lowering of permittivity, further understanding of the exact nature of these particle-matrix interactions is still required.

With increasing filler loads of TiO₂, SiO₂ and Al₂O₃, the permittivity is seen to decrease, probably due to a larger number of nanoparticles and increased available interfacial area. However, above a certain threshold load, the permittivity increases again, which is generally attributed to two possible factors.^[10, 13, 21] Firstly, with a large number of nanoparticles in closer proximity, the particles will tend to agglomerate, thereby decreasing the available interfacial

area and the number of immobilized chains. Secondly, the intrinsic polarization of the nanoparticles will begin to contribute to the effective permittivity as the particles constitute a significant volume fraction of the composite. Since the inorganic fillers have higher relative permittivities than epoxy, the permittivity of the nanocomposite will increase as well. The structure or phase of the filler may be a contributing factor here, e.g. the permittivity of TiO₂ in rutile is much larger than in anatase (Table 2).

Dielectric losses

The dielectric loss (represented by the loss tangent, $\tan \delta$) in electrical insulation materials should be low, as it will cause local dielectric heating, which may result in thermal ageing and eventually lead to breakdown. Upon addition of micron-sized particles to epoxy, an increase in the dielectric loss is generally observed at frequencies above 1 Hz.^[10, 13] If nanoparticles are used instead, a decrease in the dielectric loss is usually observed for low filler contents. The threshold filler content for a decrease in $\tan \delta$ varies between studies. The frequency dependence of $\tan \delta$ also varies significantly between studies, possibly due to differences in the temperature and electric field at which the experiments were conducted.

Singha and Thomas^[10] reported a decrease in $\tan \delta$ for epoxy nanocomposites up to 1 wt% of TiO₂ nanoparticles and an increase for 5 wt% or higher additions (at 27°C). The trends in the dielectric loss with changing frequency are the same for both neat epoxy and nanocomposites with up to 5 wt% fillers. With a higher filler content the frequency dependence changes, which indicates that the unreinforced polymer phase is no longer the dominating contribution to the permittivity.^[10] At higher frequencies (above 100 kHz) the losses decrease for all samples, but there is considerable fluctuation in the data.^[15] Nelson and Fothergill reported a decrease in $\tan \delta$ above 1 Hz for 10 wt% of TiO₂ nanoparticles (at 100°C), and showed that a reduction of the

filler content down to 1 wt% only changed the low-frequency response.^[13] No difference was seen in the frequency dependence between neat epoxy, microcomposites and nanocomposites above 10 Hz.

Measurements by Siddabattuni et al.^[4] (at room temperature and 1 kHz) showed an increase in $\tan \delta$ with the addition of 16 wt% of unmodified TiO₂ nanoparticles to epoxy. When the nanoparticles were surfaced modified using bifunctional organophosphate ligands (e.g. phenyl phosphate, aminophenyl phosphate, nitrophenyl phosphate, and chlorophenyl phosphate), the increase in $\tan \delta$ was smaller. Yeung and Vaughan reported a lower imaginary part of the relative permittivity for increasing weight ratio of GPTMS to SiO₂ nanoparticles (below 500 kHz).^[19] This corresponds to a lower $\tan \delta$ for constant real part of the permittivity.

From the findings presented above, it is observed that the use of nanoparticle fillers can reduce the dielectric losses in epoxy nanocomposites, improving its properties as electrical insulation. However, the effects of the particle sizes, filler load and surface chemistry of the filler nanoparticles (all of which affect the state of dispersion) are not well-understood and require further investigation.

4.1.2 Breakdown strength

The dielectric breakdown strength is an important parameter for electrical insulation materials, as it determines the largest electrical field stress (and consequently the maximum voltage) that can be applied to the insulation system. In addition to intrinsic materials properties, the breakdown strength also depends on the shape of the insulation, the voltage type applied (AC or DC), and the ramp rates used (among other factors).^[71] Since dielectric breakdown is a stochastic phenomenon, statistical methods are typically used to describe and predict breakdown values. Weibull probability plots are most commonly used to describe the

likelihood of dielectric breakdown in the insulation for a given electrical field strength. **Table 6** summarizes breakdown strength values of various nanocomposites from selected literature. It should be noted that different methods have been used in different studies, with respect to the type of field, ramp rates, electrodes and sample sizes. DC and AC breakdown strengths are not necessarily related or comparable quantities, but the trends in the changes in breakdown strength from the addition of nanofillers are evident.

Nelson and Fothergill reported a higher probability of breakdown at lower electric field strengths for TiO₂ microcomposites than nanocomposites (both with 10 wt% of filler particles).^[13] The nanocomposites in this study have lower breakdown strength than neat epoxy. However, the Weibull shape parameter β (slopes of the distributions) for the nanocomposites and the neat epoxy are similar, while it is noticeably different for the microcomposites. The similarity in β indicates that the origin of breakdown is similar in both nanocomposites and neat epoxy. This may also imply (but not necessarily) a similar mechanism of breakdown.^[13]

Singha and Thomas investigated the breakdown strength for epoxy nanocomposites with varying loads of TiO₂ nanofillers.^[10] Their results contradict those presented by Nelson and Fothergill. While neat epoxy still showed the highest breakdown strength, the reduction was much larger for TiO₂ nanoparticles than micron-sized particles. In addition, β changes for both micro- and nanocomposites, indicating a change in the origins of the breakdown.^[10] Imai et al.^[75] and Hu et al.^[76] conducted experiments with AC as well and reported a higher breakdown strength for TiO₂ nanocomposites than for neat epoxy. Singha and Thomas attributed the low breakdown strength of their TiO₂ nanocomposites to the large average particle sizes (50 nm

TiO₂ nanoparticles, compared to the 15 nm and 23 nm used by Imai et al.^[75] and Hu et al.^[76], respectively).

Singha and Thomas also measured the breakdown strengths of epoxy nanocomposites with Al₂O₃ (45 nm average particle size) as filler. These nanocomposites also had a lower breakdown strength than neat epoxy, but higher than the corresponding microcomposites. The authors attribute the difference in breakdown strength between the micro- and nanocomposites for the two filler types (TiO₂ and Al₂O₃) to the difference in intrinsic permittivity (TiO₂ has a significantly higher permittivity than both epoxy and Al₂O₃).^[10]

Surface modification of the filler particles generally leads to higher breakdown strength. Yeung and Vaughan^[19] reported a significant increase in the dielectric breakdown strength when GPTMS was used for surface functionalization of SiO₂ nanoparticles (2 wt%). The maximum breakdown strength was observed for a SiO₂:GPTMS mass ratio of 1:1 – further increases in the amount of SCA resulted in a decrease in the breakdown strength.^[19] Excess GPTMS can undergo a self-condensation reaction, which results in degradation of the composite properties and may lead to a lower coverage of GPTMS on the nanoparticle surface.

Siddabattuni et al.^[4] reported that epoxy-TiO₂ nanocomposites with electron-deficient ligands containing an electron-withdrawing functional group (e.g. nitrophenyl phosphate and chlorophenyl phosphate) demonstrated significantly improved breakdown strengths (up to 28% increase). A similar result was presented by Bell et al.^[23] for epoxy-SiO₂ nanocomposites (2 wt%), where the authors proposed that ligands with electron-withdrawing groups or π -conjugated small molecules act as charge carrier traps, trapping free electrons that can initiate breakdown.

Li et al. studied epoxy-Al₂O₃ nanocomposites (5 wt%, with and without GPTMS surface modification) and showed a slight increase in the breakdown strength compared to neat

epoxy.^[74] However, the surface modification did not have a significant effect on the breakdown strength in this case. This might be due to either the self-condensation of GPTMS or the difference in filler permittivity and content. An evaluation of the dispersion quality or preparing several samples with different amounts of coupling agent may assist in determining which has the most significant effect.

The effect of nanofillers on the breakdown strength can be described by considering the various mechanisms leading to electrical breakdown in the insulation. Electrical breakdown in polymers is usually a progressive process, via the formation and growth of tiny conducting channels into a tree-like structure (electrical treeing). The branches in electrical trees grow due to erosion of the polymer by partial discharges, which are initiated in regions with high electrical field stress (e.g. defects, voids, conducting particles, etc.). The accumulation or injection of space charges can also cause the inception of electrical trees by enhancing the electric field locally to above the breakdown strength.^[5, 13] Bell et al.^[23] described a different mode of breakdown initiation via an electron avalanche, which develops when electrons gain sufficient energy. When the avalanche volume reaches a critical size (200 nm), failure occurs due to large-scale bond breaking, resulting in a breakdown of the material. The model assumes that the avalanche must have sufficient energy to break all the bonds in the volume it has traveled through.

Nelson and Fothergill demonstrated a significant reduction in the amount of space charge near the electrodes in the TiO₂ nanocomposite compared to the microcomposite. The difference in the amount of space charge was corroborated by the larger maximum field intensity in microcomposites that increased with time (approximately 235 % of the applied field at the electrodes).^[13] In contrast, the electric field in nanocomposites showed less variation

(maximum of 125 % of applied field) with less local enhancement of electrical field stresses. This may have contributed to the increased breakdown strength in the nanocomposites.

Danikas and Tanaka^[71] and Li et al.^[74] proposed a different mechanism for how nanoparticles may improve the breakdown strength. In this model (represented in **Figure 11**), electrical trees propagate through the bulk polymer until they encounter a particle, which acts as a barrier. The tree must then propagate around the particle to proceed. This is supported by Tanaka's multi-core model,^[49] which proposes that partial discharges (which can initiate and help propagate electrical trees) initiate at either the outer loose layer of the interfacial region, or in the bulk polymer. These regions are more susceptible to partial discharges, while the bound and bonded layers are much more resistant. Thus, when an electrical tree propagates to the bound layer, the partial discharge activity is redirected back into the polymer or into the third layer of a neighboring nanoparticle. This results in a zig-zag pathway for the partial discharges, and the nanocomposite consequently exhibits greater resistance against electrical treeing.^[49, 71]

In addition, for the same filler load (in wt%) of micro- and nano-sized particles there will be a larger number of nanoparticles (with a larger interface) than microparticles, which will increase resistance against electrical treeing. This is consistent with the differences observed in the breakdown strengths (for epoxy nanocomposites with TiO₂) in the studies by Singha and Thomas,^[10] Imai et al.^[75] as well as Hu et al.^[76] – nanocomposites containing larger particles had lower electrical breakdown strengths. Li et al.^[74] also proposed that micron-sized particles introduce defects and voids between the particles and the polymer, which can accelerate the tree growth. Such defects and voids are shown to be smaller when nanoparticles are used,^[77] leading to an improved resistance to partial discharge activity, and possibly to improved electrical breakdown strength. In addition, since the physical size of the defects and voids close

to nanoparticles (or small agglomerates) are small, partial discharge inception will be less likely.

Several studies show that the electrical breakdown strength of epoxy nanocomposites varies for different filler contents. Singha and Thomas reported an initial decrease in the breakdown strength for epoxy-TiO₂ nanocomposites (up to 0.5 wt% of filler), followed by fluctuations in the breakdown strength with increasing filler load (up to 10 wt%). For epoxy-Al₂O₃ nanocomposites a similar behavior was observed, but the fluctuations in the breakdown strength were even smaller.^[10] In contrast, Mohanty and Srivastava^[16] show an initial increase in breakdown strength, followed by a decrease with further increasing filler content (above 4 wt%) for Al₂O₃ nanofillers. The breakdown strength still remained higher than that of epoxy after the observed decrease, contrary to the results reported by both Singha and Nelson. **Figure 12** shows agglomeration using 4 wt% Al₂O₃ compared to good dispersion using 2 wt% of Al₂O₃. The decrease in the breakdown strength can be correlated to the increased agglomeration above 4 wt% of Al₂O₃. Andritsch et al.^[21] also reported similar results as Mohanty and Srivastava for epoxy nanocomposites with Al₂O₃ as filler.

Differences in the dispersion quality are known to affect the breakdown strength. Virtanen et al.^[64] demonstrated a direct relation between the state of dispersion and dielectric breakdown strength of epoxy-SiO₂ nanocomposites with bimodal ligands. The ligands consisted of active short molecules (oligothipene and ferrocene) and PGMA chains. A decrease in the free space length (L_f) corresponded with an increase in the breakdown strength. Bell et al.^[23] demonstrated similar results by varying the graft density of the ligands (PGMA with thiophene, anthracene or terthiophene) to alter L_f . However, they report that for L_f less than 200 nm, the increases in the breakdown strength become gradually smaller. L_f is then on the scale of the critical electron

avalanche size, and the nanoparticles cannot prevent avalanches from reaching a critical size even when sufficiently well dispersed.

The electron avalanche can however be prevented from reaching a critical size by the presence of π -conjugation in the ligands, which can act as electron traps. The various ligands provide traps with different depths (based on the electronic structure), resulting in various degrees of improvement in the breakdown strength. **Figure 13** shows changes in the graft density and breakdown strength with L_f . L_f decreases with an increase in the graft density, which can also be observed from **Figure 14**, which shows a comparison of the dispersion quality for bimodal-anthracene and bimodal-thiophene grafted SiO₂ nanoparticles with different graft densities (with and without PGMA). Figure 13b shows that for bimodal-anthracene and monomodal-PGMA grafted ligands on SiO₂ nanoparticles, a significant increase in breakdown strength was observed at an L_f of approximately 200 nm, with no further increase for smaller L_f . Using bimodal-terthiophene ligands resulted in a higher breakdown strength than either of bimodal-anthracene and monomodal-PGMA ligands below L_f of 200 nm, but the data does not show if the breakdown strength also remains independent of L_f below 200 nm. Figure 14 shows a substantial improvement in the dispersion of bimodal-thiophene grafted SiO₂ upon increasing the graft density of PGMA, but the increase in the AC breakdown strength shown in Figure 13b is not as significant as those seen for the other ligands used.

The studies by Bell et al.^[23] and Siddabattuni et al.^[4] demonstrated that surface modifiers (i.e. ligands and coupling agents) may affect nanocomposites beyond simply improving the dispersion of the nanoparticles. The breakdown strength increased for ligands with electron-withdrawing groups, which could act as electron traps similar to the π -conjugated ligands.^[4] The authors stated, however, that the dispersions consisted of flocculates with an average separation in the micrometer range, varying between 700 and 1200 nm depending on the type

of surface ligands used. In this case the ligands do not contribute to improving the dispersion of the nanoparticles. The increase in breakdown strength is therefore primarily attributed to the electron traps in the ligands.^[23]

Poor dispersion or agglomeration of nanoparticles in the composite is unfavorable for the dielectric breakdown strength. This can be due to either the accumulation of space charge near the electrodes (similar to microcomposites), or the formation of large regions of the polymer without any nanoparticle reinforcement (large L_f). The accumulation of space charge near the electrodes can result in large field enhancements that can initiate breakdown,^[13] while in the regions without nanoparticle reinforcement there are no electron traps, which leads to an increased vulnerability to electrical tree growth. Therefore, it must be ensured that the dispersion of nanoparticles is homogeneous to achieve an improved breakdown strength.

4.2 Mechanical properties

Polymer composite insulation materials are subject to constant abrasion and high shear stresses, resulting in the initiation of cracks or delamination, followed by electrical discharge and failure.^[1] One of the well-known limitations of epoxy is that it is brittle, which limits application when high impact and fracture strength is required.^[78] Reinforcement of polymer matrices with inorganic or metallic filler particles is commonly used to overcome these problems and enhance the mechanical properties of the composite. Traditionally the filler particles have been micron-sized, but in the last decade the focus has shifted to nanoparticles. Nanoparticles can potentially give larger improvements of the mechanical properties of composites compared to micron-sized particles.^[79, 80] The improvements in mechanical performance are attributed to the larger surface-area-to-volume ratio for smaller particles at a

given filler load, resulting in the larger interfacial area and enhancement of the physical and chemical interactions between polymer chains and filler particles.^[60, 78] **Table 7** briefly summarizes the changes observed for selected mechanical properties of different epoxy nanocomposites (with increasing filler contents).

4.2.1 *Changes in strength and elastic moduli*

Table 7 shows that the addition of nanoparticles to epoxy generally results in improvements in the flexural and tensile strengths as well as the fracture toughness compared with neat epoxy. The enhanced strength and toughness are attributed to the particle-matrix interactions,^[61, 85] which allows uniform stress transfer from the polymer matrix to the nanoparticles.^[60, 61, 85] However, some studies have shown that excess filler loads (usually above 5-10 wt%) may result in a decrease in mechanical performance. The decrease at higher filler loads is typically attributed to the clustering of particles and the increasing particle-particle interactions due to smaller average interparticle distances (**Figure 15**).^[61, 81] These particle-particle interactions may result in uneven concentrations of stress near agglomerates, resulting in failure of the material. An increase in the elastic moduli of nanocomposites is expected due to the significantly larger elastic moduli of the inorganic nanoparticles than of epoxy.^[61, 81] Many studies use the Halpin-Tsai and Lewis-Nielsen models to compare predicted and experimental values of the tensile modulus (Figure 15c).^[61, 80, 81, 83, 85] Generally, the data shows good agreement at low filler loads with both models (using the ‘no slip’ approximation for the Lewis-Nielsen model) but larger discrepancies are seen for higher filler loads due to agglomeration effects.^[61, 80, 81, 83]

4.2.2 *Changes in the strain-to-break*

The strain-to-break represents the ductility of the material, and because neat epoxy is brittle it is preferable to increase the strain-to-break for the nanocomposites alongside the fracture toughness and tensile strength. Conflicting results have been reported for the changes in strain-to-break, with some studies showing increased values with increasing nanoparticle content (up to a certain filler content),^[60, 61] and others showing decreased values with increasing nanoparticle content.^[62, 79, 81] Zhao et al.^[81] reported that the strain-to-break increases with filler content when the nanoparticles were surface modified with a silane coupling agent (APTES). Goyat et al.^[61] reported an initial increase in the strain-to-break with increasing TiO₂ content, followed by a decrease above 7 wt% (Figure 15b,d). The results from Goyat et al. and Zhao et al. may be an indication that these properties are also dependent on the state of dispersion of the nanoparticles. The effect of the type of inorganic fillers (and their intrinsic mechanical properties) on the strain-to-break of the composite is not well established. Further studies are required to understand this effect of nanoparticles and their surface modification on the deformation of the polymer matrix and the resulting changes in brittleness.

4.2.3 Toughening mechanisms

Several different mechanisms for the toughening of epoxy by filler addition have been proposed. Crack pinning and crack deflection both increase the energy required for the crack to propagate, involving alteration of the crack path by the nanoparticles. Rigid filler particles in the epoxy can act as pinning centers, where the crack front bends outwards between the particles.^[1] However, crack pinning requires that the particles are larger than the crack-opening displacement, which is unlikely when nanoparticles are used.^[83] Wetzel et al.^[60] reported signs of crack pinning in fracture surfaces, but this may be due to the agglomeration of the nanoparticles used, which increased the effective filler particle size.

Crack deflection occurs when the crack tilts and changes direction when the crack front approaches the filler particles. Crack deflection can be observed from the fracture surfaces, as an increased surface roughness corresponds to increased crack deflection.^[61, 81, 83] However, there exist discrepancies between the experimental and predicted values for the fracture toughness, indicating that crack deflection is not solely responsible for the toughening.^[81, 83] Zhao et al.^[81] reported that the fracture surface roughness increased for surface-modified nanoparticles, which indicates that the state of dispersion may be responsible for discrepancies between the predicted and experimental data. Crack deflection also results in increased energy dissipation when the particles are well-bonded to the polymers (strong particle-matrix interface e.g. when coupling agents are used).^[61]

Another mechanism for toughening is particle debonding followed by plastic void growth. Depending on the strength of the filler-matrix interactions, the debonding process may require different amounts of energy. Johnsen et al.^[83] reported that the plastic void growth could be the main toughening mechanism for epoxy nanocomposites with unmodified SiO₂ nanoparticles. Zhao et al.,^[81] however, reported significant reduction of debonding for surface-modified Al₂O₃ particles in the hackle zones of fracture surfaces, which indicates strong interactions between the particles and the polymer chains and an increased energy requirement for debonding. Dittanet and Pearson also reported a lower fracture toughness for smaller particles at higher filler loads.^[81] Plastic void growth was also observed in other studies where the presence of voids are not the sole toughening mechanisms.^[60, 61]

4.3 Thermal properties

The temperature and thermal stability of polymer nanocomposites can have drastic effects on their structure and behavior. These effects should be considered when selecting the materials

for various applications, particularly in high voltage insulation where dielectric losses result in heat dissipation, raising the temperature of the material. The thermal stability of the materials is important, as exposure to high temperatures eventually results in degradation of material properties via thermal decomposition.

4.3.1 Changes in the glass transition temperature

The glass transition temperature (T_g) is the temperature above which polymers transition from a hard, glassy state to a viscous, rubbery state, resulting in changes of the physical properties of the material. The exact determination of T_g from these methods varies subjectively since the transition occurs over a temperature range, and therefore different studies may yield different numerical results. In addition, T_g depends on the type and load of filler nanoparticles used, and also on whether they are surface functionalized or not. The transition may also be affected by various other factors, such as the molecular weight of the polymer chains, polymer tacticity, the cross-linking density and the type of curing agent or hardener used.^[10, 19, 61] **Table 8** shows selected ranges for T_g for different epoxy-based nanocomposites. A wide spread in the results is seen, with T_g for neat epoxy varying between 65 and 222°C. As seen from Table 8, there is no consensus between different studies on the effect of nanoparticle fillers on the glass transition temperature of epoxy. In nanocomposites for high-voltage insulation applications a larger T_g is favorable because it enables higher operational temperatures. Dittanet and Pearson^[85] and Goyat et al.^[61] showed a small decrease in T_g upon addition of small amounts of nanoparticles (SiO_2 and TiO_2 respectively), and then an increase with increasing filler load. Singha and Thomas^[10] reported similar behavior for TiO_2 and Al_2O_3 nanoparticles, although the nanocomposites with the highest filler loads (10 wt%) still showed a slightly smaller T_g than neat epoxy. Lizundia et al.^[87] reported increases in T_g both when the SiO_2 particles were

surface modified with cross-linked epoxy-amine, and also when smaller particles (15 nm) were used. Larger SiO₂ particles (>70 nm) with no surface modification showed decreased T_g with increasing filler loads. Siddabattuni et al.^[4] reported a large decrease in T_g when TiO₂ nanoparticles were used, but upon surface modification with various bifunctional organophosphate ligands T_g increased again. On the other hand, both Zhao et al.^[81] and Yeung and Vaughan^[19] showed a small decrease in T_g when the nanoparticles were surface modified. Several studies have highlighted the importance of the interactions between the filler and the polymer matrix on T_g. Lizundia et al.^[87] attributed the increase in T_g to improved compatibility between the particles and the matrix due to the surface modification (cross-linked epoxy-amine). In addition, TEM showed reduced agglomeration and significantly improved dispersion of the nanoparticles when they were surface modified. Goyat et al.^[61] proposed that improved particle-matrix interactions resulted in the immobilization of the polymer chains when the particles were well-dispersed. A larger amount of energy will be needed to overcome these interactions and mobilize the chains during the glass transition, hence T_g will increase. Further, for higher filler loads, T_g decreased significantly, which corresponded with larger cluster sizes and therefore, poorer dispersion. This proposed effect of the nanoparticles impeding the chain mobility is also used to explain changes in the relative permittivity of nanocomposites, as discussed in **Chapter 4.1.1**. Singha and Thomas also proposed that the nature of the interactions at the interface between nanoparticles and polymer may influence T_g, and that the state of dispersion affects these interfacial phenomena.^[10]

Yeung and Vaughan^[19] discuss the differences between their results and the changes in T_g predicted by the chain immobilization model. T_g decreased slightly with increasing filler loads – however, the changes in T_g did not vary systematically with the composition, and the authors concluded that this invariance in the range of T_g indicated that there are no interfacial regions

with filler-matrix interactions affecting the chain dynamics in the bulk polymer. Yeung and Vaughan also highlighted results from Nguyen et al.,^[59] which showed that T_g does vary systematically with changing stoichiometric ratio of epoxy to anhydride (hardener).

Zhang et al.^[62] reported a unique case where epoxy-SiO₂ nanocomposites showed a second glass transition temperature (T_β), which behaved differently from T_g . T_β increased with increasing filler load, whereas T_g decreased. However, no mechanism was proposed for the occurrence of T_β . Interestingly, the appearance of this second glass transition is predicted by the Tsagaropoulos model for the interface (**Chapter 2.3**), which attributes this glass transition to the loosely bound interfacial layer.^[48] The strongly bound first layer does not participate in the glass transition due to the impeded chain mobility.^[43] However, no other reports of this second glass transition have been found in literature for epoxy nanocomposites.

4.3.2 *Changes in thermal conductivity and thermal stability*

There is less focus in literature on the effect of inorganic oxide fillers on the thermal conductivity or thermal stability of epoxy nanocomposites. Increasing the thermal conductivity of nanocomposites, compared with that of neat epoxy, will be advantageous for high voltage insulation applications. Lower thermal conductivity results in larger temperature gradients in the insulation for DC applications, which cause larger gradients in the electrical conductivity and increases the electric field stress near the conductor. In addition, low thermal conductivity limits the power rating of the electrical component, meaning less current density is transferred through the conductors. An increased thermal stability will also be beneficial, as higher temperatures will be required to degrade the material, improving the operating temperature range in applications.

Kochetov et al.^[26] reported an increased thermal conductivity with increasing filler loads for SiO₂, Al₂O₃, MgO and AlN nanoparticles. This increase is anticipated, as the thermal conductivities of ceramics are higher than that of epoxy (Table 1 and Table 2). Micron-sized particles of SiO₂ and Al₂O₃ have the same effect as nanoparticles. Due to their higher thermal conductivities, the inorganic fillers are proposed to act as pathways for heat transfer while the epoxy acts as a thermal barrier.^[26] For a given filler load, composites with microparticles have higher thermal conductivities than those with nanoparticles. Kochetov et al. attributed this effect to phonon scattering on the larger surface area of nanoparticles, but this cannot be determined conclusively.^[26] Xie et al.^[25] investigated the changes in thermal conductivity for epoxy nanocomposites with TiO₂ nanoparticles and nanowires. The thermal conductivity increased with increasing filler load in both cases, but the increase was larger for nanowires. The authors suggested that this was due to the aspect ratio of the nanowire. A longer nanowire is more beneficial for heat transfer than spherical nanoparticles as they form thermally conductive channels.^[25]

The thermal stability of epoxy-based composites is observed to increase when inorganic oxide nanoparticles are incorporated, but there are some discrepancies in the results reported in literature. **Table 9** summarizes the changes in the initial degradation temperature (IDT), the temperature required for 5 % mass loss in the material, which is often used as an indicator for the thermal stability. Ghosh et al.^[88] reported increased stability of epoxy-TiO₂ nanocomposites with an increase in the IDT, which is attributed to the cross-linking ability of the TiO₂ nanoparticles. However, further increases in the TiO₂ content led to a decrease in the IDT, which was attributed to inhomogeneous dispersion of the nanoparticles. On the other hand, Xie et al.^[25] showed a decrease in the IDT for epoxy-TiO₂ nanocomposites. One possible explanation for this discrepancy may be that the nanoparticles used by Xie et al. are larger (60

nm) than those used by Ghosh et al. (50 nm). Arabli and Aghili^[89] reported a small increase in the IDT for epoxy nanocomposites containing SiO₂, which is corroborated by Liu et al.^[91] However, Alzina et al.^[90] presented the opposite, showing decreased thermal stability with a lower IDT. Guo et al.^[57] showed small changes in the thermal stability dependent on the type of surface modification used. It is worth noticing that the studies showing increased thermal stability used SiO₂ nanoparticles that are smaller in size (10-20 nm)^[89, 91] than those used in the study showing decreased stability (above 50 nm).^[90] This indicates a possible trend where the thermal stability increases with decreases in the nanoparticle size. However, the variations in the results may also be attributed to differences in the fabrication procedures, and the reactants or solvents used. Additionally, in some studies^[57, 88, 91] the thermogravimetric data show a plateau-like region between 400 and 600 °C where the decomposition of the nanocomposites is slowed down, which is attributed to the decomposition of benzene rings.^[57] However, in other studies^[16, 25, 89, 90] the data show only a single thermal decomposition step, with no plateau. The effect of small concentrations of nanoparticles on the thermal stability of the epoxy nanocomposites is therefore not yet well understood, and requires further investigation.

5. Conclusions and Outlook

There have been promising developments over the last decade showcasing the benefits of epoxy nanocomposites for high voltage insulation applications. Although there is room for further improvement in our understanding of the material system and its functionalities, some consistent observations and trends can be outlined. Surface functionalization of the inorganic filler nanoparticles with silane coupling agents is seen to improve the dispersion of the nanoparticles, which is linked to lower permittivities and dielectric losses. Surface functionalization with ligands containing electron-withdrawing groups is seen to improve the

dielectric breakdown strength of the nanocomposite. The mechanical strengths and elastic moduli of epoxy are also increased by the inclusion of nanoparticles. However, the effect of the nanoparticles on the glass transition temperature is not well understood so far. Generally, it is observed that agglomeration of the nanoparticles or an otherwise poor state of dispersion will lead to deterioration of the properties desired for application in high voltage insulation systems. Of several potential quantitative methods to characterize the state of dispersion, the free space length method seems the most promising.

An increased focus on the interactions at the interfaces between filler and matrix may lead to a better description of the structure-property relations in nanocomposites, and is suggested for future studies in the field. Improvements in the processing techniques and preparation methods to improve the dispersion quality should be prioritized. The use of quantitative methods to characterize the state of dispersion is strongly recommended, to allow comparison between different samples with minimal subjective bias.

5.1 Characterization of the interface

A thorough investigation of the nature of the interactions at the interfaces can improve the understanding of several different phenomena, particularly the diverse changes of the dielectric properties and the glass transition temperature. Several characterization techniques are available that provide chemical and physical information of the nanoparticles, their surface functionalities, and the coupling agent chemistry.^[1] These different techniques may be implemented together in future studies to provide a better description of the nature of the interactions at interfaces in nanocomposites.

Fourier Transform Infrared (FTIR) and Raman spectroscopy can be used to probe the nanoparticle surfaces and characterize the functional groups and chemical structure of the

coupling agents or ligand molecules.^[1, 83] FTIR is a standard method to characterize the nanoparticle surface before and after surface modification.^[7, 19, 20, 61] Small-angle X-ray scattering (SAXS) and dynamic light scattering (DLS) can be used to study the effective thickness of the surface modification layer and the nanoparticle dispersions and size distributions.^[92, 93] X-ray photoelectron spectroscopy (XPS) gives information about the surface chemistry and bonding of the nanoparticles.^[1, 92]

Ab initio modeling techniques, such as density functional theory (DFT), are suitable to gain additional fundamental understanding of the electronic structure of polymer nanocomposites.^[92] The electronic structure at the interfaces is important due to the offsets between the valence and conduction bands in the two different insulators (filler and matrix). Interface and defect states can act as electron traps (accomplished by energy dissipation via electron-phonon interactions), potentially improving the dielectric breakdown strength.^[1] An investigation of the various interfaces, interface states and phonons may help to explain the difference in characteristics (e.g. breakdown strength, T_g) of nanocomposites compared to neat epoxy. *Ab initio* methods may also allow one to describe the properties of the interfacial regions that cannot be determined experimentally, using multiscale models. Recently, Kim et al. investigated the thermomechanical properties (Young's modulus and coefficient of thermal expansion (CTE)) of the interfacial regions in epoxy-SiO₂ nanocomposites using *ab initio* molecular dynamics (MD) and molecular mechanics (MM) simulations.^[94]

5.2 Improvement of nanoparticle dispersion

There is a strong indication that maximizing the interactions between polymer and inorganic filler leads to improvements in the electrical and mechanical properties of the nanocomposites. Calebrese et al.^[14] demonstrated that the processing parameters, which determine the state of

particle dispersion, must be well controlled to avoid variations in the dielectric behavior. Surface functionalization is found to be advantageous for the complex permittivity and breakdown strength, and is strongly recommended based on the findings presented here. The use of surface ligands with electron traps^[4, 23, 64] provides interesting possibilities in addition to the more conventional silane coupling agents, and should be investigated further. Alternative mixing techniques should also be attempted in order to improve the dispersion quality, as high shear mixing may not break up all the agglomerated nanoparticles. Kurimoto et al.^[22] demonstrated a reduction in agglomerate size with ultrasonication and centrifugal mixing, but this method lacks control of the filler content after processing.

It is strongly recommended that quantitative techniques are used to analyze the state of dispersion, rather than relying on a qualitative assessment. As discussed earlier in **Section 3.2**, there are advantages and disadvantages of the various quantitative measures of dispersion, and in some cases it may be optimal to combine several quantitative analysis techniques. The benefit of a quantitative assessment is that it provides parameters for describing the state of dispersion and can facilitate comparison of the dispersion quality in different materials, while removing subjective user interpretation.^[14, 65] A quantitative assessment will also make it easier to assess the impact of different preparation and processing methods on the dispersion, and subsequently the properties of the material.

5.3 Future outlook

The literature presents a promising avenue for the application of epoxy-based nanocomposites for high voltage insulation materials. The use of inorganic oxide nanoparticles provides not only mechanical reinforcement (as done traditionally using micron-sized particles), but can

also improve the dielectric breakdown strength while decreasing dielectric loss and relative permittivity of the material. One of the main challenges is to obtain homogeneous dispersion without agglomerated nanoparticles, which may require new and innovative techniques for successful achievement. Comprehension of the nature of interactions between filler and matrix, as well as the significance of the interfacial region, will require a multidisciplinary approach, combining the fields of chemistry, materials science, physics, electrical engineering and statistics. Achieving this understanding of the fundamental structure-property relations will open up new possibilities to tailor these hybrid materials for various applications in nanodielectrics.

Acknowledgements

This work is funded by The Research Council of Norway through the project "Stipendiatstillinger til SINTEF Energi AS" (Project No. 259866).

Received: ((will be filled in by the editorial staff))

Revised: ((will be filled in by the editorial staff))

Published online: ((will be filled in by the editorial staff))

References

- [1] J. K. Nelson, *Dielectric Polymer Nanocomposites*, Springer, New York, USA **2010**.
- [2] T. Tanaka, G. C. Montanari, R. Mulhaupt, *IEEE Trans. Dielect. Electr. Insul.* **2004**, *11*, 763.
- [3] T. Tanaka, *IEEE Trans. Dielect. Electr. Insul.* **2005**, *12*, 914.
- [4] S. Siddabattuni, T. P. Schuman, F. Dogan, *ACS Appl. Mater. Interfaces* **2013**, *5*, 1917.
- [5] I. Plesa, P. V. Notingher, S. Schlögl, C. Sumereder, M. Muhr, *Polymers* **2016**, *8*.
- [6] H. Zou, S. Wu, J. Shen, *Chem. Rev.* **2008**, *108*, 3893; P. H. C. Camargo, K. G. Satyanarayana, F. Wypych, *Mat. Res.* **2009**, *12*, 1.

This is the peer reviewed version of the following article: Adnan, Mohammed Mostafa, et al. "Epoxy-Based Nanocomposites for High-Voltage Insulation: A Review." *Advanced Electronic Materials* (2018): 1800505, which has been published in final form at <https://doi.org/10.1002/aelm.201800505>. This article may be used for non-commercial purposes in accordance with Wiley Terms and Conditions for Use of Self-Archived Versions

- [7] J. Jiao, P. Liu, Y. Cai, *J. Polym. Res.* **2013**, 20.
- [8] D. Liu, G. He, X. A. Zeng, D. W. Sun, X. Li, *Polym. Compos.* **2014**, 35, 1388; Y.-T. Bi, Z.-J. Li, W. Liang, *Polym. Adv. Technol.* **2013**, 25, 173.
- [9] Z. Han, R. Garrett, *Nanotechnology* **2008**, 2, 727; R. Sarathi, R. K. Sahu, P. Rajeshkumar, *Mater. Sci. Eng., A* **2007**, 445-446, 567.
- [10] S. Singha, M. J. Thomas, *IEEE Trans. Dielect. Electr. Insul.* **2008**, 15, 12.
- [11] W. D. Callister Jr., D. G. Rethwisch, *Callister's Materials Science and Engineering*, Wiley India, India **2010**.
- [12] T. Imai, F. Sawa, T. Ozaki, T. Shimizu, S. Kuge, T. Tanaka, *IEEJ Trans. Fundam. Mater.* **2006**, 126, 84.
- [13] J. K. Nelson, J. C. Fothergill, *Nanotechnology* **2004**, 15, 586.
- [14] C. Calebrese, L. Hui, L. S. Schadler, J. K. Nelson, *IEEE Trans. Dielect. Electr. Insul.* **2011**, 18, 938.
- [15] S. Singha, M. J. Thomas, *IEEE Trans. Dielect. Electr. Insul.* **2008**, 15, 2.
- [16] A. Mohanty, V. K. Srivastava, *Mater. Des.* **2013**, 47, 711.
- [17] M. Iijima, S. Takenouchi, W. Lenggoro, H. Kamiya, *Adv. Powder Technol.* **2011**, 22, 663; S. Mallakpour, M. Dinari, *Mater. Res. Bull.* **2013**, 48, 3865; S. Mallakpour, M. Hatami, *Polym. Plast. Technol. Eng.* **2012**, 51, 1106; F. Ahangaran, A. Hassanzadeh, S. Nouri, *Nano Lett.* **2013**, 32, 1.
- [18] C. Zou, J. C. Fothergill, S. W. Rowe, *IEEE Trans. Dielect. Electr. Insul.* **2008**, 15, 106.
- [19] C. Yeung, A. S. Vaughan, *Polymers* **2016**, 8.
- [20] R. Kochetov, T. Andritsch, P. H. F. Morshuis, J. J. Smit, *IEEE Trans. Dielect. Electr. Insul.* **2012**, 19, 107.
- [21] T. Andritsch, R. Kochetov, P. H. F. Morshuis, J. J. Smit, in *Annual Report Conference on Electrical Insulation and Dielectric Phenomena*, **2010**.
- [22] M. Kurimoto, H. Okubo, K. Kato, M. Takei, Y. Hoshina, M. Hanai, N. Hayakawa, *IEEE Trans. Dielect. Electr. Insul.* **2010**, 17, 1268; M. Kurimoto, H. Okubo, K. Kato, M. Takei, Y. Hoshina, M. Hanai, N. Hayakawa, *IEEE Trans. Dielect. Electr. Insul.* **2010**, 17, 662.
- [23] M. Bell, T. Krentz, J. K. Nelson, L. Schadler, K. Wu, C. Breneman, S. Zhao, H. Hillborg, B. Benicewicz, *J. Colloid Interface Sci.* **2017**, 495, 130.
- [24] I. A. Tsekmes, P. H. F. Morshuis, J. J. Smit, *IEEE Elect. Insul. Mag.* **2015**, 31, 32; Y. J. Kim, T. S. Shin, H. D. Choi, J. H. Kwon, Y.-C. Chung, H. G. Yoon, *Carbon* **2005**, 43, 23.

- [25] Q. Xie, Y. Cheng, S. Chen, G. Wu, Z. Wang, Z. Jia, *J. Mater. Sci. Mater. Electron.* **2017**, *Published online*.
- [26] R. Kochetov, A. V. Korobko, T. Andritsch, P. H. F. Morshuis, S. J. Picken, J. J. Smit, *J. Phys. D* **2011**, *44*, 395401.
- [27] K. Kowalczyk, T. Spychaj, *Prog. Org. Coat.* **2008**, *62*, 425.
- [28] T. Zhu, S.-P. Gao, *J. Phys. Chem. C* **2014**, *118*, 11385.
- [29] A. Boonchun, P. Reunchan, N. Umezawa, *Phys. Chem. Chem. Phys.* **2016**, *18*, 30040.
- [30] D. Reyes-Coronado, G. Rodriguez-Gattorno, M. E. Espinosa-Pesquera, C. Cab, R. de Coss, G. Oskam, *Nanotechnology* **2008**, *19*, 145605; T. A. Kandiel, A. Feldhoff, L. Robben, L. Dillert, D. W. Bahnemann, *Chem. Mater.* **2010**, *22*, 2050.
- [31] M. Dou, C. Persson, *J. Appl. Phys.* **2013**, *113*, 083703.
- [32] K. Momma, F. Izumi, *J. Appl. Crystallogr.* **2011**, *44*, 1272.
- [33] C. J. Howard, T. M. Sabine, F. Dickson, *Acta Crystallogr.* **1991**, *B47*, 462; L. Pauling, J. H. Sturdivant, *Z. Kristallogr. Cryst. Mater.* **1928**, *68*.
- [34] H. Zhang, D. R. Dunphy, X. Jiang, H. Meng, B. Sun, D. Tarn, M. Xue, X. Wang, S. Lin, Z. Ji, R. Li, F. L. Garcia, J. Yang, M. L. Kirk, T. Xia, J. I. Zink, A. Nel, C. J. Brinker, *J. Am. Chem. Soc.* **2012**, *134*, 15790.
- [35] I. Levin, D. Brandon, *J. Am. Chem. Soc.* **1998**, *81*, 1995.
- [36] A. H. Tavakoli, P. S. Maram, S. J. Widgeon, J. Rufner, K. van Benthem, S. Ushako, S. Sen, A. Navrotsky, *J. Phys. Chem. C* **2013**, *117*, 17123.
- [37] U. Chowdhry, A. W. Sleight, *Annu. Rev. Mater. Res.* **1987**, *17*, 323.
- [38] J. F. Shackelford, W. Alexander, *CRC Materials Science and Engineering Handbook*, CRC Press, **2001**.
- [39] A. I. Kingon, J.-P. Maria, S. K. Streiffer, *Nature* **2000**, *406*, 1032.
- [40] G. D. Wilk, R. M. Wallace, J. M. Anthony, *J. Appl. Phys.* **2001**, *89*, 5243.
- [41] D. Liu, S. J. Clark, J. Robertson, *Appl. Phys. Lett.* **2010**, *96*, 032905.
- [42] N. H. Ismail, M. Mustapha, *Polymer Engineering and Science* **2018**, *Published online*.
- [43] T. Heid, M. Fréchet, E. David, *Journal of Materials Science* **2015**, *50*, 5494.
- [44] T. Heid, M. Fréchet, E. David, *IEEE Trans. Dielect. Electr. Insul.* **2015**, *22*, 1176.
- [45] T. Tanaka, Y. Matsuo, K. Uchida, in *Annual Report Conference on Electrical Insulation Dielectric Phenomena*, IEEE, Quebec, QC, Canada **2008**, 13.

- [46] C. N. R. Rao, P. J. Thomas, G. U. Kulkarni, *Nanocrystals: Synthesis, Properties and Applications*, Springer-Verlag Berlin Heidelberg, Berlin, Germany **2007**.
- [47] W. R. Caseri, in *Nanocomposites: In situ synthesis of polymer-embedded nanostructures*, (Eds: L. Nicolais, G. Catotenuto), John Wiley and Sons, Hoboken, NJ, USA **2014**, 45.
- [48] G. Tsagaropoulos, A. Eisenberg, *Macromolecules* **1995**, 28, 6067.
- [49] T. Tanaka, M. Kozako, N. Fuse, Y. Ohki, *IEEE Trans. Dielect. Electr. Insul.* **2005**, 12, 669.
- [50] T. J. Lewis, *IEEE Trans. Dielect. Electr. Insul.* **2004**, 11, 739.
- [51] S. Kango, S. Kalia, A. Celli, J. Njugana, Y. Habibi, R. Kumar, *Prog. Polym. Sci.* **2013**, 38, 1232.
- [52] S. Mallakpour, M. Madani, *Prog. Org. Coat.* **2015**, 86, 194.
- [53] S. P. Pujari, L. Scheres, A. T. M. Marcelis, H. Zuilhof, *Angew. Chem. Int. Ed.* **2014**, 53, 6322.
- [54] H. Gu, C. Ma, J. Gu, J. Guo, X. Yan, J. Huang, Q. Zhang, Z. Guo, *J. Mater. Chem. C* **2016**, 4, 5890.
- [55] C. Lü, B. Yang, *J. Mater. Chem.* **2009**, 19, 2884.
- [56] A. R. M. Dalod, *PhD thesis: In situ synthesis of titania and titanium based organic-inorganic nanomaterials*, Norwegian University of Science and Technology (NTNU), Norway **2017**.
- [57] Q. Guo, P. Zhu, G. Li, J. Wen, T. Wang, D. Lu, R. Sun, C. Wong, *Composites Part B* **2017**, 116, 388.
- [58] Q. Shi, L. Wang, H. Yu, S. Jiang, Z. Zhao, X. Dong, *Macromolecular Materials and Engineering* **2006**, 291, 53.
- [59] V. T. Nguyen, A. S. Vaughan, P. L. Lewin, A. Krivda, *IEEE Trans. Dielect. Electr. Insul.* **2015**, 22, 895.
- [60] B. Wetzell, F. Hauptert, M. Q. Zhang, *Compos. Sci. Technol.* **2003**, 63, 2055.
- [61] M. S. Goyat, S. Rana, S. Halder, P. K. Ghosh, *Ultrason. Sonochem.* **2018**, 40, 861.
- [62] H. Zhang, Z. Zhang, K. Friedrich, C. Eger, *Acta Materiala* **2006**, 54, 1833.
- [63] M. S. Goyat, S. Ray, P. K. Ghosh, *Composites: Part A* **2011**, 42, 1421.
- [64] S. Virtanen, T. Krentz, J. K. Nelson, L. Schadler, M. Bell, B. Benicewicz, H. Hillborg, S. Zhao, *IEEE Trans. Dielect. Electr. Insul.* **2014**, 21.

- [65] L. Hui, R. C. Smith, X. Wang, J. K. Nelson, L. S. Schadler, in *Annual Report Conference on Electrical Insulation Dielectric Phenomena*, IEEE, Quebec, Canada **2008**, 317.
- [66] H. S. Khare, D. L. Burris, *Polymer* **2010**, *51*, 719.
- [67] D. Kim, J. S. Lee, C. M. F. Barry, J. L. Mead, *Microscopy Research and Technique* **2007**, *70*, 539.
- [68] Z. P. Luo, J. H. Koo, *Mater. Lett.* **2008**, *62*, 3493; Z. P. Luo, J. H. Koo, *Journal of Microscopy* **2007**, *225*, 118; Z. P. Luo, J. H. Koo, *Polymer* **2008**, *49*, 1841.
- [69] M. Morisita, *Mem. Fac. Sci. Kyushu Univ. Ser. E* **1959**, *3*, 65.
- [70] Q. Wang, G. Chen, A. S. Alghamdi, in *International Conference on Solid Dielectrics*, IEEE, Potsdam, Germany **2010**.
- [71] M. G. Danikas, T. Tanaka, *IEEE Elect. Insul. Mag.* **2009**, *25*, 19.
- [72] G. Iyer, R. S. Gorur, R. Richert, A. Krivda, L. E. Schmidt, *IEEE Trans. Dielect. Electr. Insul.* **2011**, *18*, 659.
- [73] M. Liang, K. L. Wong, *Energy Procedia* **2017**, *110*, 162.
- [74] Z. Li, K. Okamoto, Y. Ohki, T. Tanaka, *IEEE Trans. Dielect. Electr. Insul.* **2010**, *17*, 653.
- [75] T. Imai, F. Sawa, T. Ozaki, Y. Inoue, T. Shimizu, T. Tanaka, in *IEEE Conference on Electrical Insulation and Dielectric Phenomena*, Kansas City, MO, USA **2006**, 306.
- [76] Y. Hu, R. C. Smith, J. K. Nelson, L. S. Schadler, in *IEEE Conference on Electrical Insulation and Dielectric Phenomena*, Kansas City, MO, USA **2006**, 31.
- [77] N. Fuse, Y. Ohki, M. Kozako, T. Tanaka, *IEEE Trans. Dielect. Electr. Insul.* **2008**, *15*.
- [78] D. Pinto, L. Bernardo, A. Amaro, S. Lopes, *Construction and Building Materials* **2015**, *95*, 506.
- [79] I. Ozsoy, A. Demirkol, A. Mimaroglu, H. Unal, Z. Demir, *Strojniški vestnik - Journal of Mechanical Engineering* **2015**, *61*, 601.
- [80] Y. L. Liang, R. A. Pearson, *Polymer* **2009**, *50*, 4895.
- [81] S. Zhao, L. S. Schadler, R. Duncan, H. Hillborg, T. Auletta, *Compos. Sci. Technol.* **2008**, *68*, 2965.
- [82] P. Carballeira, F. Hauptert, *Polym. Compos.* **2010**, *31*, 1241.
- [83] B. B. Johnsen, A. J. Kinloch, R. D. Mohammed, A. C. Taylor, S. Sprenger, *Polymer* **2007**, *48*, 530.
- [84] Y. Zheng, Y. Zheng, R. Ning, *Mater. Lett.* **20053**, *57*, 2940.

- [85] P. Dittanet, R. A. Pearson, *Polymer* **2012**, *53*, 1890.
- [86] C. J. Huang, S. Y. Fu, Y. H. Zhang, B. Lauke, L. F. Li, L. Ye, *Cryogenics* **2005**, *45*, 450.
- [87] E. Lizundia, I. Serna, E. Axpe, J. L. Vilas, *Journal of Applied Polymer Science* **2017**, *134*, 45216.
- [88] P. K. Ghosh, A. Pathak, M. S. Goyat, S. Halder, *J. Reinf. Plast. Compos.* **2012**, *31*, 1180.
- [89] V. Arabli, A. Aghili, *Adv. Compos. Mater* **2015**, *24*, 561.
- [90] C. Alzina, N. Sbirrazuoli, A. Mija, *J. Phys. Chem. C* **2011**, *115*, 22789.
- [91] Y.-L. Liu, C.-Y. Hsu, W.-L. Wei, R.-J. Jeng, *Polymer* **2003**, *44*, 5159.
- [92] M. A. Boles, D. Ling, T. Hyeon, D. V. Talapin, *Nature Materials* **2016**, *15*, 141.
- [93] C. Becker, B. Kutsch, H. Krug, H. Kaddami, *Journal of Sol-Gel Science and Technology* **1998**, *13*, 499.
- [94] B. Kim, J. Choi, S. Yang, S. Yu, M. Cho, *Composites Part B* **2017**, *120*, 128.

Figures

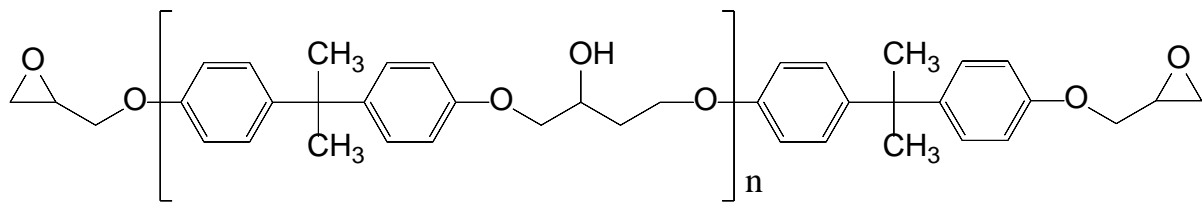


Figure 1. Structure of polymer formed from diglycidyl ether of bisphenol-A

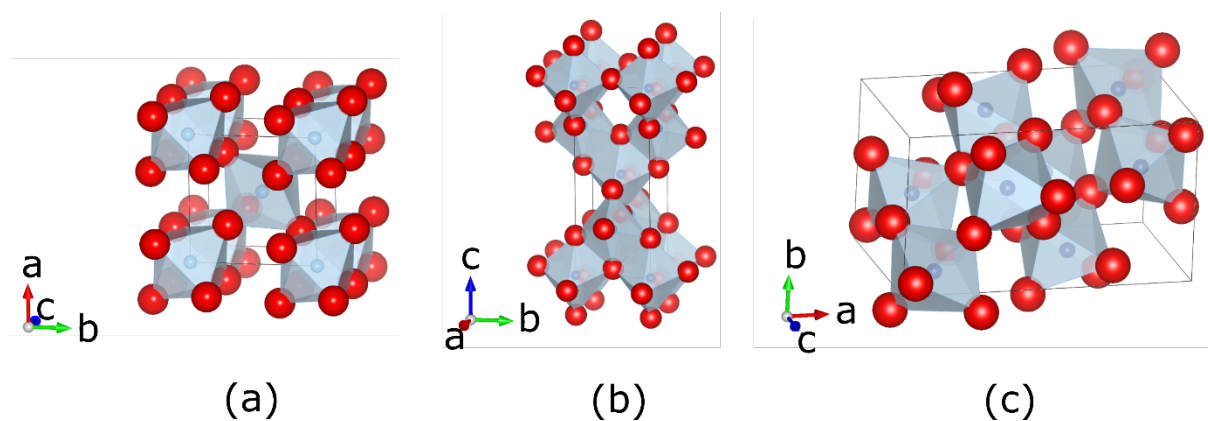


Figure 2. Crystal structures of the three polymorphs of TiO_2 : (a) rutile, (b) anatase, and (c) brookite. Figures were drawn using VESTA^[32] with atomic positions from Howard et al.^[33] The O ions are red spheres, Ti ions are blue spheres.

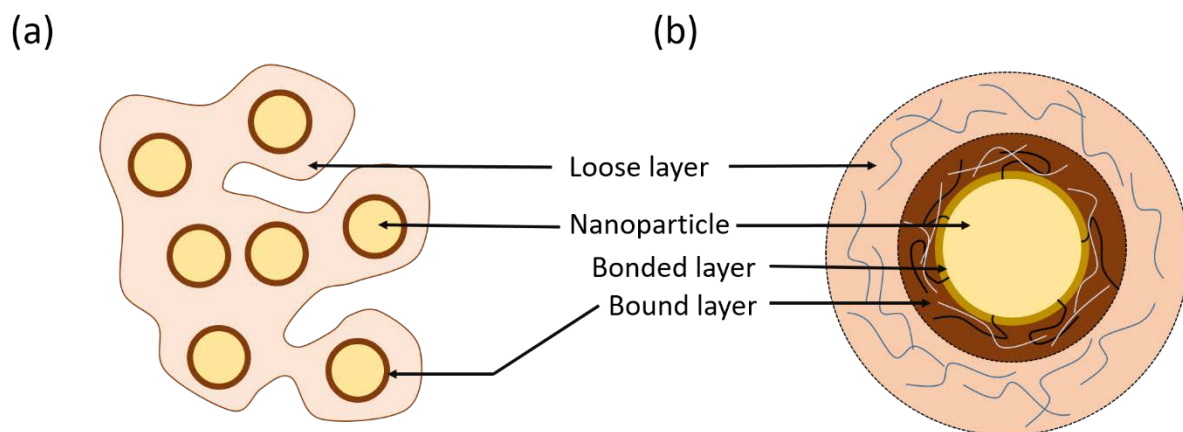


Figure 3. Representations of the two models of the interfaces between nanoparticles and the polymer matrix: (a) Double layer region model from Tsagaropoulos and Eisenberg,^[48] and (b) multi-core model from Tanaka et al.^[49]

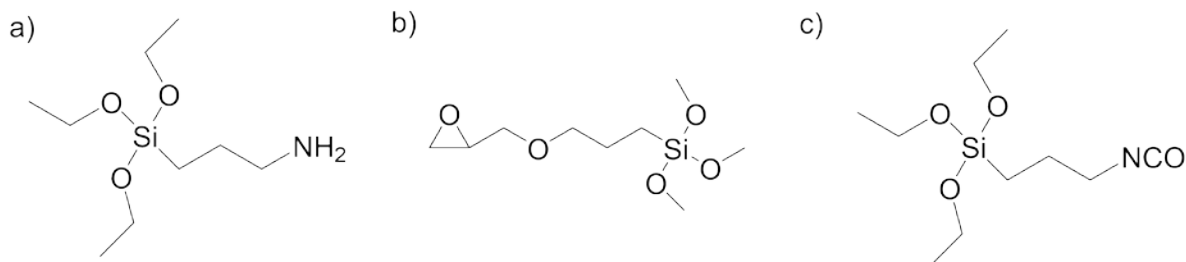


Figure 4. Chemical representations of different silane coupling agents: (a) APTES, (b) GPTMS, and (c) IPTES.

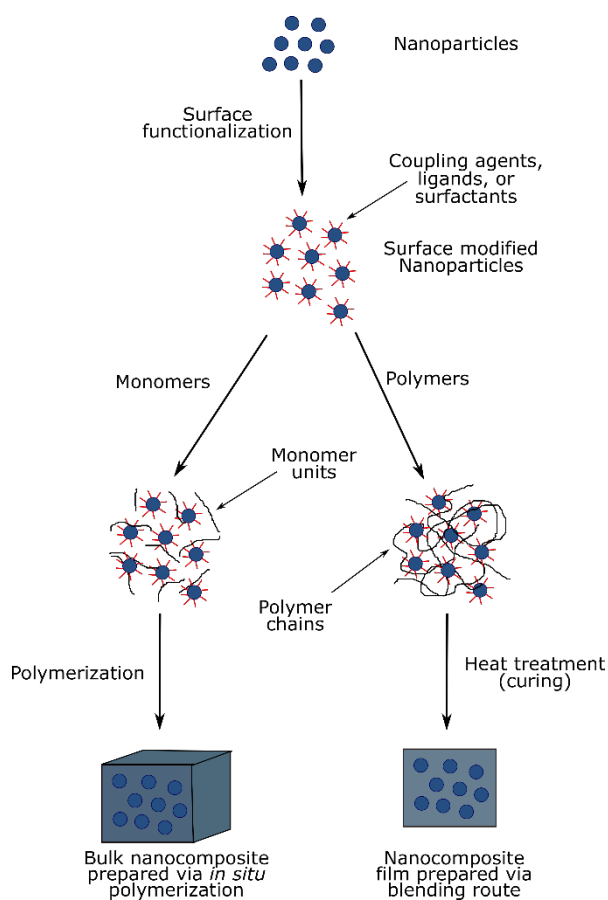


Figure 5. The schematic shows the two *ex situ* synthesis procedures used in the fabrication of epoxy nanocomposites, with *in situ* polymerization after mixing the nanoparticles with monomer units (left), or blending the nanoparticles with the polymer chains (right).

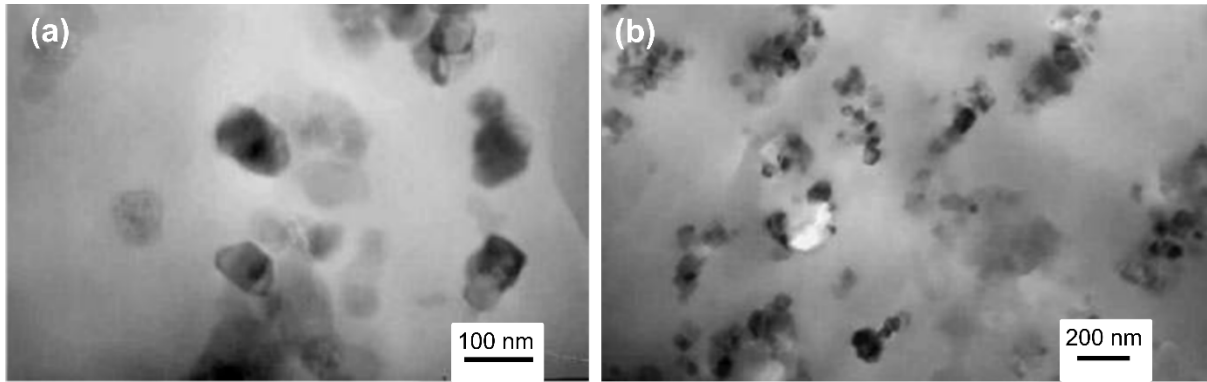


Figure 6. TEM images of an epoxy nanocomposite with 15 wt% of CaCO_3 prepared by (a) *in situ* polymerization, and (b) solution blending, showing the difference in the nanocomposite morphology due to the fabrication procedure. The TEM images are adapted with permission.^[58] 2006, WILEY-VCH Verlag GmbH & Co.

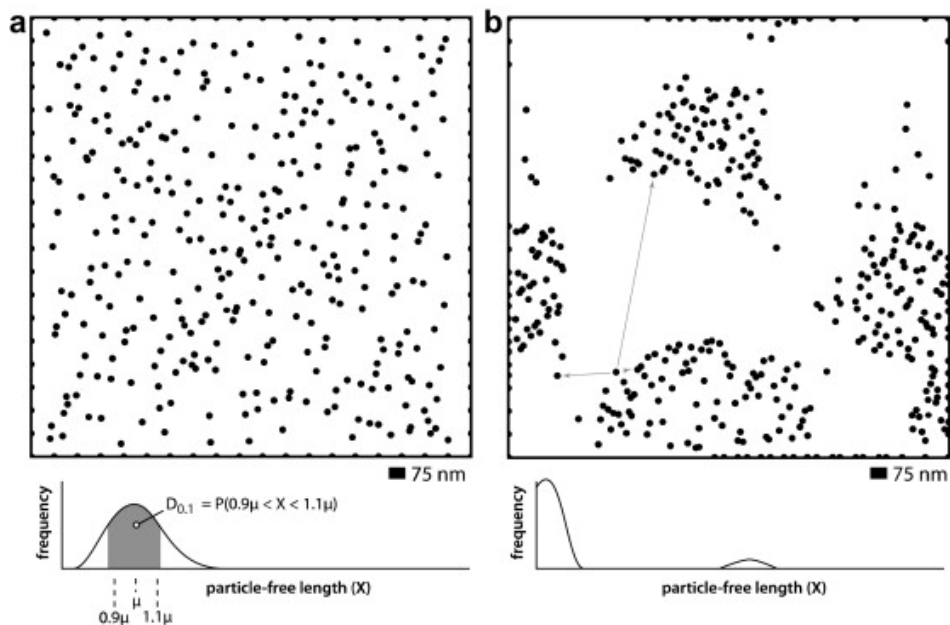


Figure 7. Hypothetical dispersions with the same average interparticle distance: (a) random dispersion of nanoparticles, and (b) agglomerated nanoparticles. The histograms below the dispersions show the distributions of the measured interparticle distances. Reprinted with permission.^[66] 2009, Elsevier Ltd.

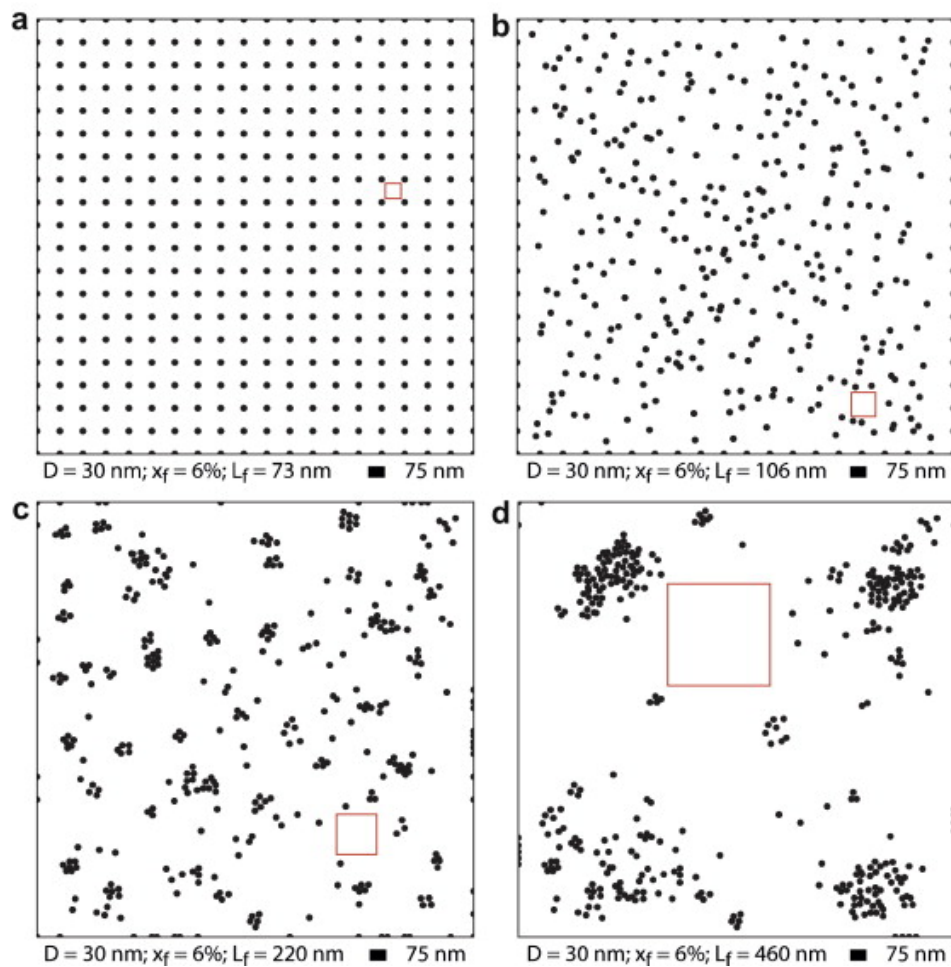
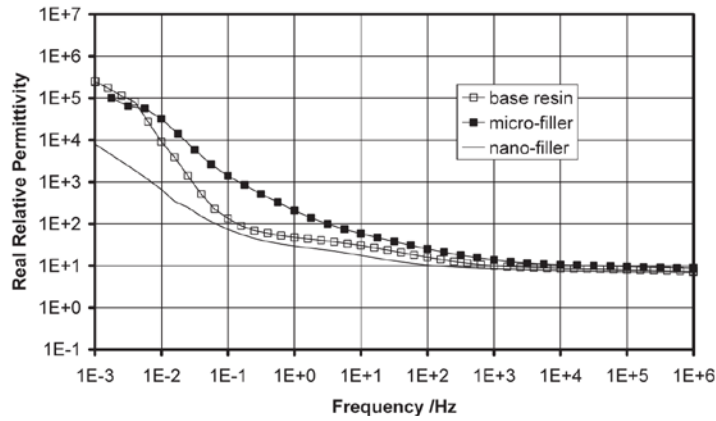
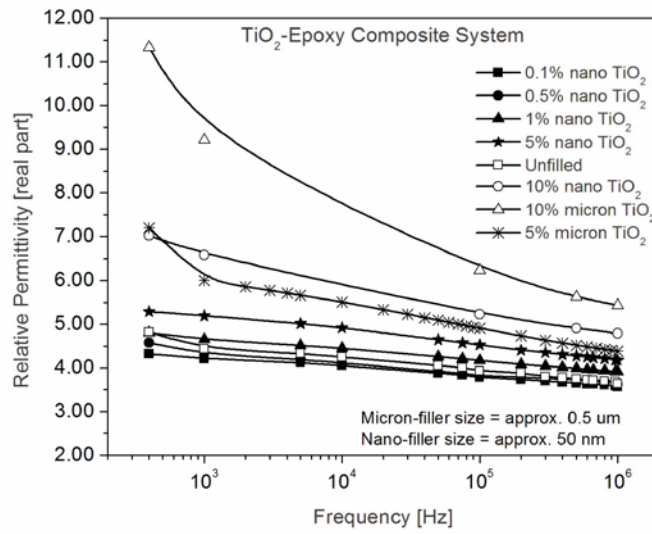


Figure 8. Varying hypothetical dispersions (constant filler load and particle size) of nanoparticles with increasing L_f as the dispersion quality decreases: (a) uniform dispersion (ideal), (b) random dispersion, (c) dispersion with small agglomerates, and (d) Dispersion with large agglomerates. L_f is given by the length of one side of the red squares. Reprinted with permission.^[66] 2009, Elsevier Ltd.



(a)



(b)

Figure 9. Comparison of the changes in relative permittivity for epoxy composites with nano and micron-sized TiO_2 particles from (a) Nelson and Fothergill (10 wt%) (reproduced with permission,^[13] 2004, IOP Publishing Ltd.), and (b) Singha and Thomas (0.1 – 10 wt%) (reproduced with permission,^[10] 2008, IEEE). Note that the frequency ranges are different in (a) and (b).

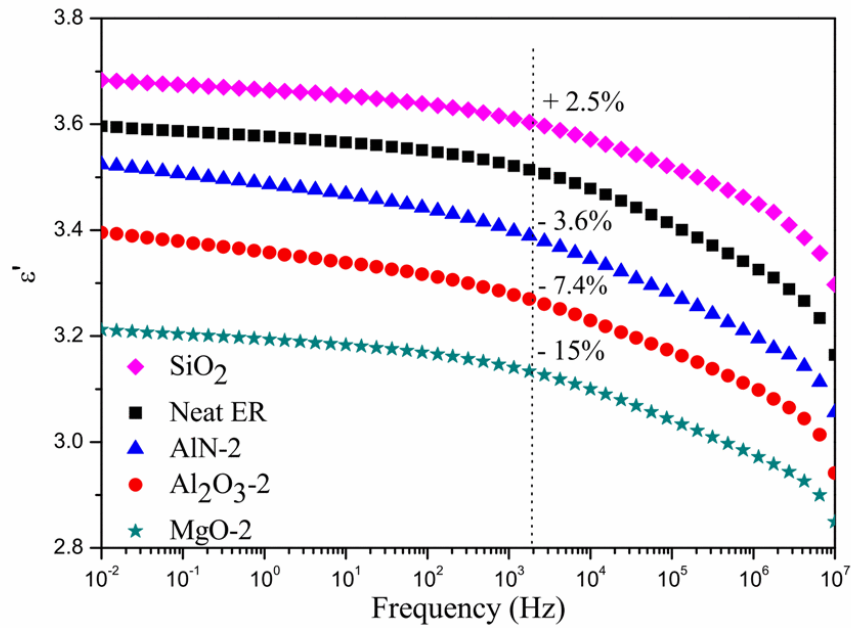


Figure 10. Relative permittivity as a function of frequency for different filler types (2 wt% filler load) in epoxy. Reproduced with permission.^[20] 2012, IEEE.

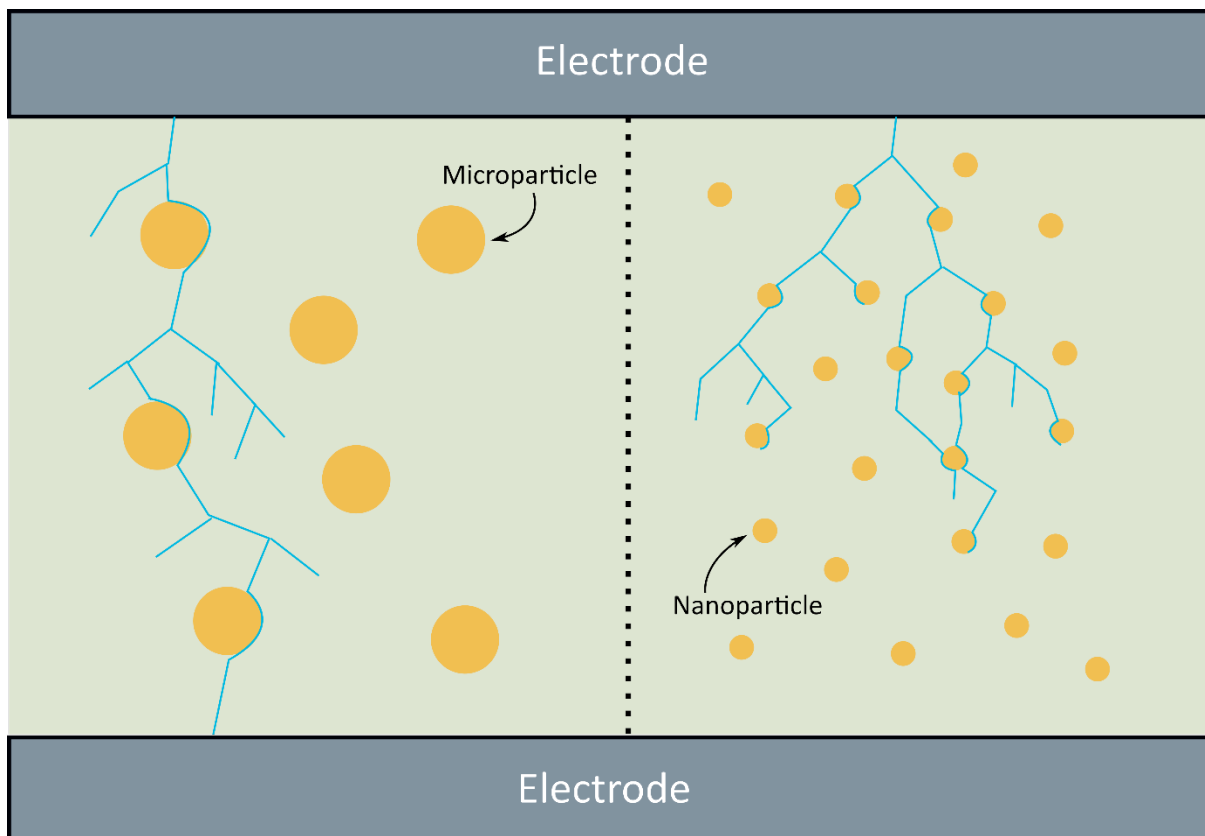


Figure 11. Electrical tree propagation (blue lines) in epoxy composites with micro and nano-sized filler particles (left and right respectively).

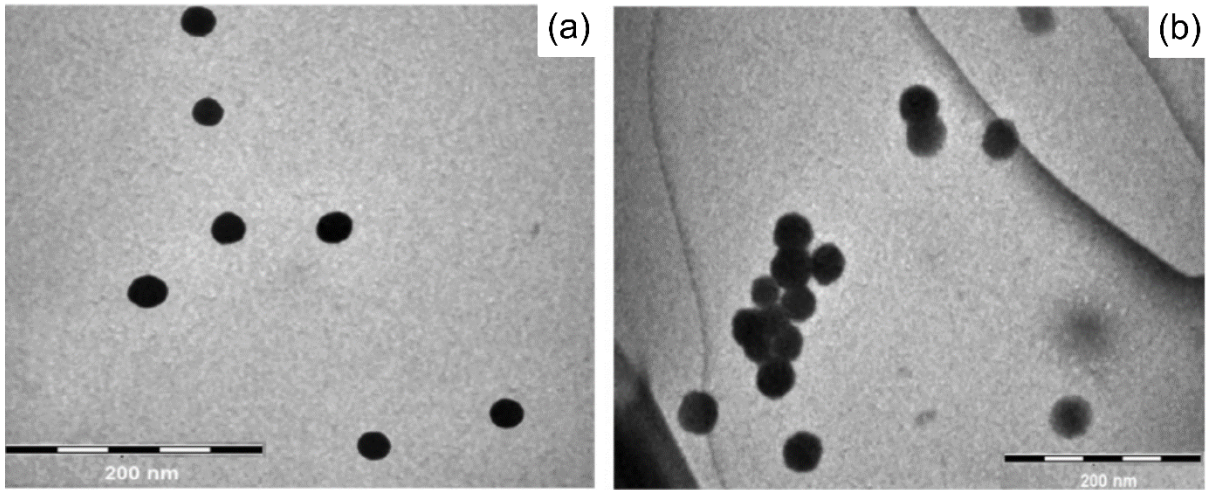


Figure 12. TEM images of epoxy composites containing (a) 2 wt%, and (b) 4 wt% of Al_2O_3 . Adapted with permission.^[16] 2012, Elsevier Ltd.

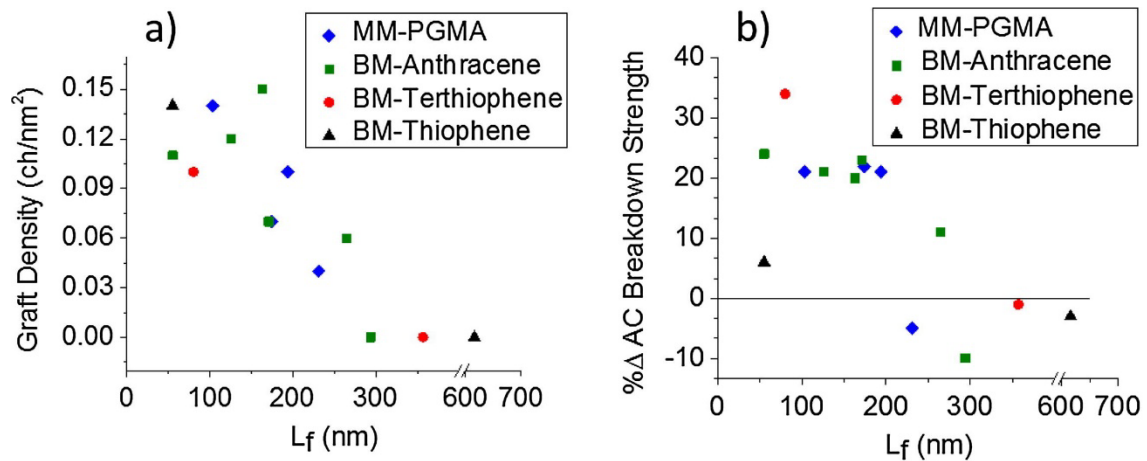


Figure 13. Changes in (a) graft density, and (b) breakdown strength, versus the free space length (L_f) for four different ligands used for SiO_2 nanoparticles (2 wt%) in epoxy (BM = bimodal, MM = monomodal, PGMA = polyglycidyl methacrylate). Adapted with permission.^[23] 2017, Elsevier Inc.

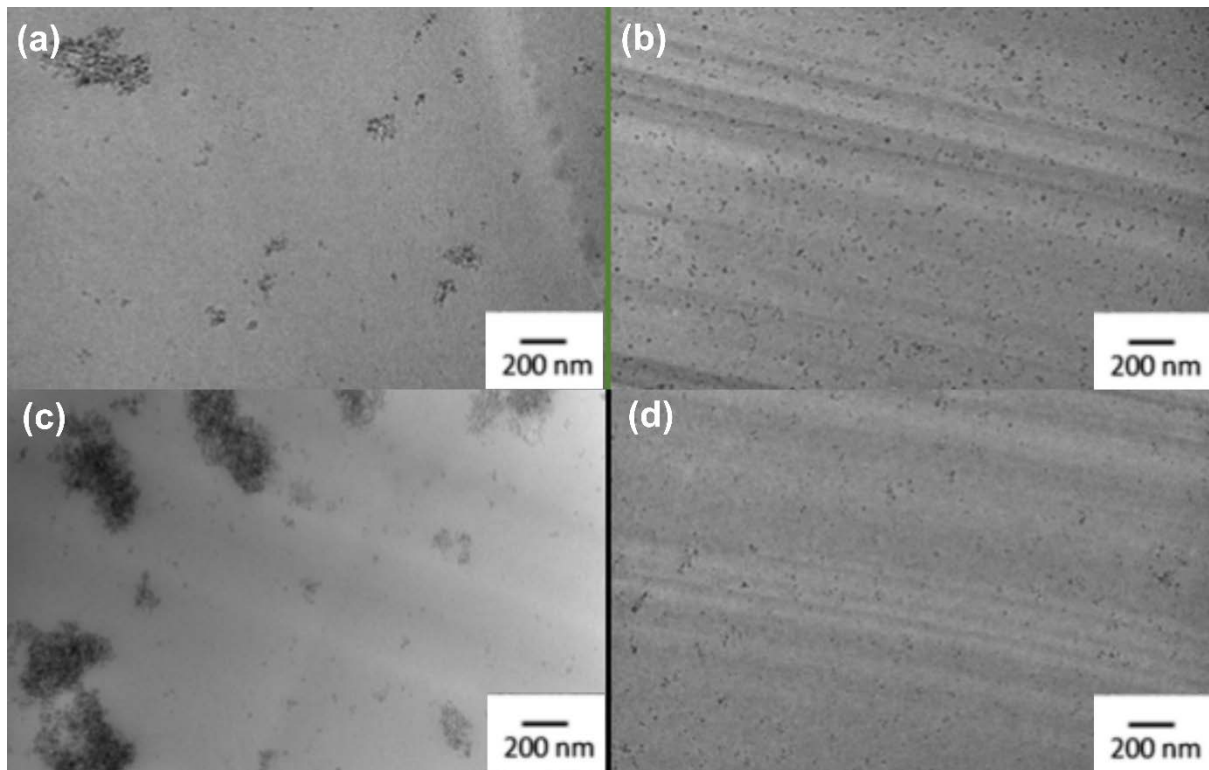


Figure 14. TEM images used for comparing the dispersion quality for BM-anthracene grafted SiO₂ nanoparticles (a) with PGMA chains ($L_f = 294$ nm), and (b) without PGMA chains ($L_f = 126$ nm), and BM-thiophene grafted SiO₂ nanoparticles (c) with PGMA chains ($L_f = 616$ nm), and (d) without PGMA chains ($L_f = 55$ nm). Adapted with permission.^[23] 2017, Elsevier Inc.

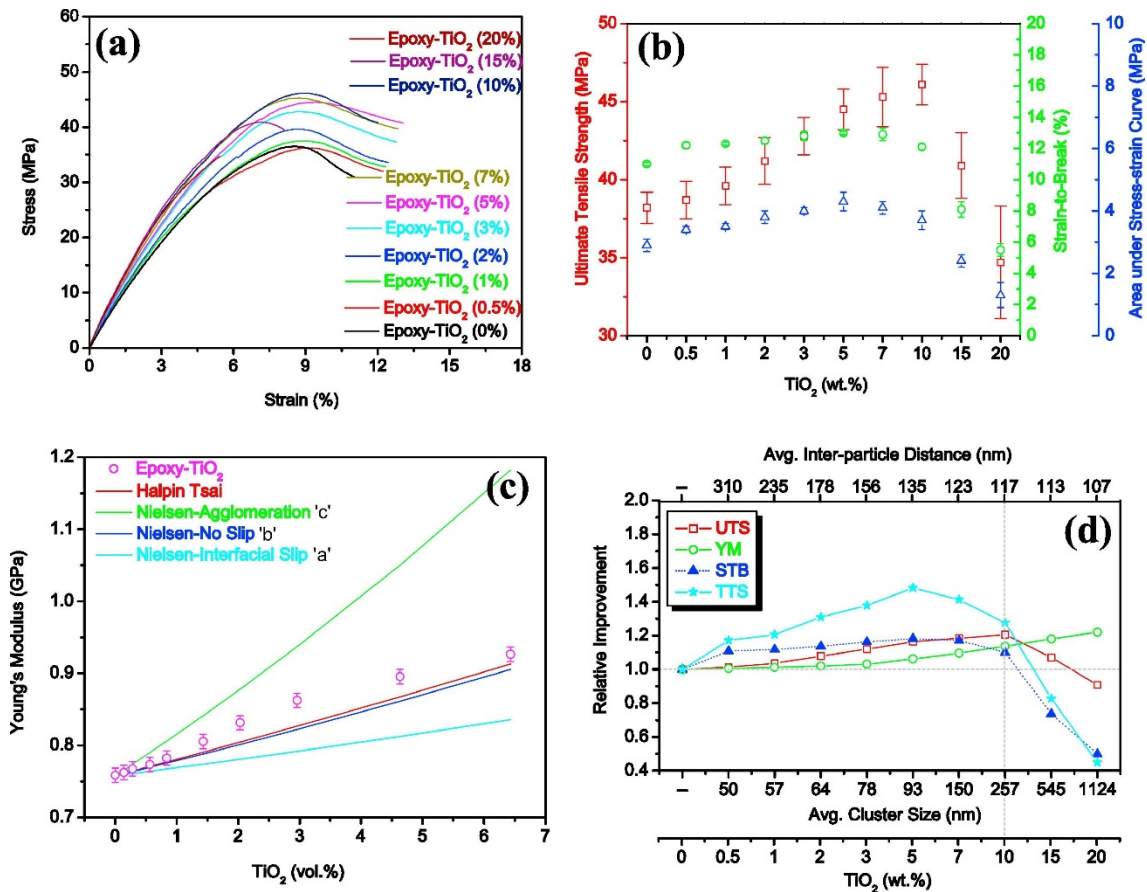


Figure 15. (a) Stress-strain curves of various epoxy-TiO₂ nanocomposites, (b) variations in selected tensile properties with nanofiller content, (c) variation in theoretical and experimental elastic moduli with nanofiller content, and (d) relative improvement of the ultimate tensile strength (UTS), Young's modulus (YM), strain-to-break (STB) and tensile toughness (TTS) as a function of nanofiller content, average cluster size, and average interparticle distance. Reprinted with permission.^[61] 2017, Elsevier B.V.

Tables

Table 1. Properties of DGEBA epoxy

Property	Approximate Values ^{a)}	References
Relative permittivity (50 Hz)	3-5 ^{b)}	19-22
Glass transition temperature (°C)	72-99	4, 7, 10
Dielectric breakdown strength (kV mm ⁻¹)	185-288	4, 13, 23
Electrical conductivity (S m ⁻¹)	~10 ⁻¹⁶ -10 ⁻¹⁵	24
Thermal conductivity (W m ⁻¹ K ⁻¹)	0.1 – 0.5	5, 25, 26
Buchholz Hardness	80 – 104	27

^{a)} Affected by curing conditions and chain length (equivalent epoxide weight); ^{b)} Nelson and Fothergill^[13] report permittivity above 10 at 50 Hz.

Table 2. Selected properties for the TiO₂, SiO₂ and Al₂O₃ filler materials.

Filler		Relative Permittivity ^{a)}	Band gap (eV)	Thermal conductivity (W m ⁻¹ K ⁻¹) ^{b)}
TiO ₂	Rutile	70 – 170 ^[1, 31]	3.34 ^[28]	6.69 – 7 ^[37, 38]
	Anatase	23 – 45 ^[31]	3.56 ^[28]	
SiO ₂ (amorphous)		2.3 – 3.9 ^[1, 39]	8.9 ^[40]	0.8 – 2 ^[37, 38]
Al ₂ O ₃	Corundum	9 ^[1]	8.8 ^[41]	25 ^[38]
	Amorphous		6.4 ^[41]	

^{a)} Frequency unspecified (assumed to be static values); ^{b)} Bulk values at room temperature.

Table 3. Synthesis methods for epoxy nanocomposites from selected literature.

Epoxy type	Filler type	Filler load	Dispersion Method	Surface modification	References
Bisphenol-A	SiO ₂	0-10 wt%	Mechanical shear mixing	Nanopox ^{b)}	20
		5 wt%		Unspecified silane treatment	12
		2 wt%		Surface modification by ligand engineering	23
		2 wt%	Mechanical mixing, then ultrasonication	GPTMS for surface functionalization	19
		0-10 wt%		Nanopox	59
	Al ₂ O ₃	0-10 wt%	Mechanical shear mixing	GPTMS for surface functionalization	20
		0-10 wt%	Mechanical shear mixing, then ultrasonication	No surface modification ^{c)}	10
		0.5-10 vol%	Mechanical shear mixing	No surface modification ^{c)}	60
		0-10 wt%	Ultrasonication	GPTMS for surface functionalization	21
		0.5 vol%	Ultrasonication, followed by centrifugal force	Unspecified SCA used	22
	TiO ₂	10 wt%	Unstated, implied to be mechanical mixing	No surface modification ^{c)}	13
		0-20 wt%	High speed impeller stirring, then ultrasonication	No surface modification ^{c)}	61
		0-10 wt%	Mechanical shear mixing, then ultrasonication	No surface modification ^{c)}	10, 15
Cycloaliphatic epoxy ^{a)}	SiO ₂	0-23 wt%	Mechanical mixing	No surface modification. SiO ₂ was obtained pre-dispersed in epoxy (40 wt%)	62

^{a)}3,4-Epoxy cyclohexylmethyl-3,4-epoxycyclohexanecarboxylate epoxy resin; ^{b)}Nanopox is a commercially available dispersion of 40 wt% SiO₂ in bisphenol-A epoxy with unknown surface modifications; ^{c)}The authors do not modify the particle surfaces, but it is unknown whether they have been pre-modified by the supplier.

Table 4. Selected methods for quantitative analysis of the state of dispersion of nanoparticles in nanocomposites.^[65-67]

Method	Principle behind method	Notes
Interparticle distance	Average of distances between particles	Scale-dependent method. Sensitive to number of particles. Poor indicator of particle distribution.
	Distribution of distances between particles	Scale-independent method. Independent of particle density. Indicates size of unreinforced polymer.
Particle density	Average number of particles per unit area	May misinterpret the dispersion due to large agglomerates. Can be combined with the Morisita index to provide spatial distribution of particles.
Skewness-Quadrat	Number of particles in each equally sized cell of a region	Skewness is sensitive to quadrat size and shape. Standard normalization method required for comparison between different filler loads.
Free space length (L_f)	Size of largest, randomly placed square with high probability of containing zero nanoparticles.	Represents characteristic size of unreinforced polymer domains. Reflects idealized trends in nanofillers dispersion, size and load. Sensitive to agglomeration size if agglomerates are as large as L_f

Table 5. Comparison of the effect of different filler types and loads on relative permittivity (at 1 kHz), from Kochetov et al.^[20]

Filler	Average particle size (nm)	Filler load (wt%)	Intrinsic relative permittivity of nanoparticle	Change in permittivity of nanocomposite from neat epoxy (%)
Al ₂ O ₃	30	0.5	11	-3.3
		2		-7.4
		5		-2.0
MgO	22	0.5	9.7	-12.1
		2		-15.0
		5		-10.9
AlN	60	0.5	8.8	-2.2
		2		-3.6
		5		+1.9
SiO ₂ ^{a)}	20	0.5	3.8	+1.6
		2		+2.5
		5		+4.5

^{a)}The SiO₂ nanoparticles were pre-dispersed in epoxy with unknown surface modifications. The other nanoparticles were surface-modified using GPTMS.

Table 6. Summary of the effect of nanoparticles on the breakdown strength for epoxy-based nanocomposites.

Filler	Filler load	Measurement of breakdown characteristics	Change in breakdown voltage compared to neat epoxy (%)	Reference		
TiO ₂	10 wt%	Weibull scale parameter (α) from ramp DC voltage	500 V s ⁻¹ ramp rate	-9.7	13	
	~16 wt% ^{a)}		200 V s ⁻¹ ramp rate	-14.2 – 27.8 ^{b)}	4	
	5 wt% 10 wt%	Weibull scale parameter (α) from ramp AC voltage	500 V s ⁻¹ ramp rate	-42.4 -33.9	10	
SiO ₂	2.5 wt% 5 wt%		1 kV s ⁻¹ ramp rate	0.6 -0.7	72	
	2 wt% ^{a)}		500 V s ⁻¹ ramp rate	13.5 – 48.7 ^{b)}	23	
	2 wt% ^{a)}		Unknown	21.9 – 48.1 ^{b)}	64	
	1 wt%		1 kV s ⁻¹ ramp rate	3.7	73	
	2 wt% ^{a)}		50 V s ⁻¹ ramp rate	30.8 – 47.3 ^{b)}	19	
	Al ₂ O ₃		0.5 wt% 5 wt%	Weibull scale parameter (α) from ramp DC voltage	-23.6 -28.9	10
0.5 wt% ^{a)} 5 wt% ^{a)}			500 V s ⁻¹ ramp rate		61.3 40.6	21
4 wt% 10 wt%			Average breakdown voltage from ramp AC		133.3 83.3	16
5 wt% ^{a)}			Weibull scale parameter (α) from ramp AC voltage		4.5	74

^{a)} Nanoparticles have been surface modified; ^{b)} Depending on the surface modification of the nanoparticles

Table 7. Changes in mechanical properties of epoxy nanocomposites with various fillers from selected literature.

Measured property	Filler	Change in property with increasing filler content	Reference
Flexural modulus	Al ₂ O ₃	Increased	60
		Increased (up to 5 wt%)	79
	TiO ₂	Increased	79
	SiO ₂	Increased	62
Flexural strength	Al ₂ O ₃	Increased	60
		Increased (up to 5 wt%)	79
	TiO ₂	Increased	79
	SiO ₂	Decreased slightly	62
Flexural strain-to-break	Al ₂ O ₃	Increased (up to 2 wt%)	60
		Decreased	79
	TiO ₂	Decreased	79
	SiO ₂	Decreased	62
Tensile modulus	Al ₂ O ₃	Increased	79
		Increased both with and without surface modification. Increase was greater without surface modification.	81
	TiO ₂	Increased	61
		Increased	79
		Increased	82
	SiO ₂	Increased	83
		Increased (up to 3 wt%)	84
Increased		85	
Tensile strength	Al ₂ O ₃	Increased (up to 2.5 wt%)	79
		Increased for unmodified nanoparticles. No change (up to 15 wt%) for surface modified nanoparticles ^{a)} , followed by large decrease	81
	TiO ₂	Increased (up to 10 wt%)	61
		Increased (up to 2.5 wt%)	79
		Increased	82
	SiO ₂	Increased (up to 2 wt%). Greatly increased at lower temperatures	86
		Increased (up to 3 wt%)	84
Tensile strain-to-break	Al ₂ O ₃	Decreased	79
		Decreased for unmodified nanoparticles. Increased (up to 15 wt%) for surface modified nanoparticles ^{a)}	81
	TiO ₂	Increased (up to 5 wt%)	61
		Decreased	79
Fracture toughness	SiO ₂	Increased	62
		Increased	83
		Increased	80

		Increased	85
Impact energy and wear resistance	Al ₂ O ₃	Increased (up to 6.7 wt%)	60
Tensile toughness	TiO ₂	Increased (up to 5 wt%)	61
Impact strength		Increased (up to 3 wt%)	84
Fracture energy	SiO ₂	Increased	83
		Increased	85

a) APTES used for surface modification of the Al₂O₃ nanoparticles

Table 8. Comparison of glass transition temperatures for selected epoxy nanocomposites from literature. Neat epoxy is indicated when filler type is left blank.

Material		Temperature (°C)	Method	Notes	Reference
Filler type	Filler Load (wt%)				
- SiO ₂	- 2.5 – 30	80.1 79.2 – 82.8	DSC	T _g increases with increasing filler content	85
- TiO ₂	- 0 – 10	65 62 – 80	DSC	T _g decreases for higher filler loads	61
- SiO ₂	- 0 – 9	91 87.5 – 96	DSC	Changes in T _g dependent on particle size and surface modification	87
- - SiO ₂ SiO ₂	- - 0 – 20 0 – 20	143 153 137 – 141 150 – 152	DSC DMTA DSC DMTA	Irregular changes in T _g , no consistent trend observed	83
- Al ₂ O ₃	- 0 – 10	112 101 – 112	DSC	T _g decreased only when particles were surface modified with APTES	81
- SiO ₂	- 2	80.5 74 – 81.5	DSC	T _g decreased with increasing amount of surface modification (GPTMS)	19
- TiO ₂	- ~16	99 85 – 100	DSC	Dependent on type of ligand used for surface modification	4
- TiO ₂ Al ₂ O ₃	- 0 – 10 0 – 5	70 61 – 69 61 – 68	DSC	Initial decrease in T _g followed by increase with increasing filler load	10
- SiO ₂	- 0 – 24	82 77 – 88	DSC	T _g increased with increasing filler load upto ~12 wt%. Irregular changes with smaller particles	80
- - SiO ₂ SiO ₂	- - 0 – 23 0 – 23	191 222 184 – 197 209 – 222	DSC DMTA DSC DMTA	T _g decreased with increasing filler load, but quite irregularly ^{a)}	62

^{a)}A second glass transition temperature was observed (T_β) that increased with increasing filler load.

Table 9: Comparison of the IDT for epoxy nanocomposites with various filler contents.

Filler	Filler content (wt%)	IDT (°C)	Reference
TiO ₂	0	256	88
	4	273	
	10	302	
	15	274	
	20	295	
TiO ₂	0	337.3	25
	4	267.7	
Al ₂ O ₃	0	310	16
	1	317	
	3	305	
	5	302	
SiO ₂	0	387	89
	4	390	
SiO ₂	0	355	90
	10	345	
SiO ₂	0	360	57
	10	~360 ^{a)}	
SiO ₂	0	250	91
	10	255	

^{a)}Sensitive to the type of surface modification used